Genome-Wide Transcript Profiling of Endosperm without Paternal Contribution Identifies Parent-of-Origin–Dependent Regulation of *AGAMOUS-LIKE36*

Reza Shirzadi[1], Ellen D. Andersen[1], Katrine N. Bjerkan[1], Barbara M. Gloeckle[2], Maren Heese[2], Alexander Ungru[3], Per Winge[4], Csaba Koncz[5,6], Reidunn B. Aalen[1], Arp Schnittger[2,3], Paul E. Grini[1]*

1 Department of Molecular Biosciences (IMBV), University of Oslo, Oslo, Norway, 2 Department of Molecular Mechanisms of Phenotypic Plasticity, Institut de Biologie Moléculaire des Plantes (IBMP), UPR2357 du CNRS, Université de Strasbourg, Strasbourg, France, 3 Unigruppe am Max-Planck-Institute for Plant Breeding Research, Department of Botany III, University of Cologne, Cologne, Germany, 4 Department of Biology, Norwegian University of Science and Technology, Trondheim, Norway, 5 Max-Planck-Institute for Plant Breeding Research, Cologne, Germany, 6 Institute of Plant Biology, Biological Research Center of Hungarian Academy of Sciences, Szeged, Hungary

Abstract

Seed development in angiosperms is dependent on the interplay among different transcriptional programs operating in the embryo, the endosperm, and the maternally-derived seed coat. In angiosperms, the embryo and the endosperm are products of double fertilization during which the two pollen sperm cells fuse with the egg cell and the central cell of the female gametophyte. In *Arabidopsis*, analyses of mutants in the cell-cycle regulator *CYCLIN DEPENDENT KINASE A;1* (*CKDA;1*) have revealed the importance of a paternal genome for the effective development of the endosperm and ultimately the seed. Here we have exploited *cdka;1* fertilization as a novel tool for the identification of seed regulators and factors involved in parent-of-origin–specific regulation during seed development. We have generated genome-wide transcription profiles of *cdka;1* fertilized seeds and identified approximately 600 genes that are downregulated in the absence of a paternal genome. Among those, *AGAMOUS-LIKE* (*AGL*) genes encoding Type-I MADS-box transcription factors were significantly overrepresented. Here, *AGL36* was chosen for an in-depth study and shown to be imprinted. We demonstrate that *AGL36* parent-of-origin–dependent expression is controlled by the activity of METHYLTRANSFERASE1 (MET1) maintenance DNA methyltransferase and DEMETER (DME) DNA glycosylase. Interestingly, our data also show that the active maternal allele of *AGL36* is regulated throughout endosperm development by components of the FIS Polycomb Repressive Complex 2 (PRC2), revealing a new type of dual epigenetic regulation in seeds.

Introduction

Seed development is a tightly regulated process that is controlled, both before and after fertilization and requires tight coordination of parental gene expression [1]. A paradigm for the importance of balanced parental contribution is the observation that certain genes in the developing offspring of flowering plants are exclusively or preferentially expressed from only one of the two parental genomes, a phenomenon called genomic imprinting that has also been observed in mammals [2,3]. The relevance of parent-of-origin effects was first found in interploidy crosses [4]. Typically, an increase in the paternal genome results in larger seeds, while the opposite is observed if the maternal gene dosage is higher than normal [5]. This is in agreement with the parental conflict theory, which implies that fathers direct maximal amount of maternal resources to their own offspring and thereby promote growth. Mothers on the other hand would seek to distribute the resources equally among all their offspring, and balance their resource between themselves and their offspring. Thus, maternal factors are thought to dampen growth [6].

In mammals, imprinted genes are often involved in growth control [7–10]. In *Arabidopsis*, the endosperm is the major tissue regulating the flow of nutrients to the embryo, and is therefore a likely site for parent-of-origin dependent gene expression.

Imprinting results from differences in epigenetic marks, involving DNA methylation and post-translational modifications of histones on the parental alleles [11,12]. Trimethylation of lysine 27 on histone H3 (H3K27me3) leading to repression of gene expression, has been found to be a particularly important imprinting mechanism in plants. In *Arabidopsis* seeds, H3K27me3 mark is set by the FIS Polycomb Repressive Complex 2 (PRC2), which consists of at least four components; the histone methyl-

Author Summary

Seeds of flowering plants consist of three different organisms that develop in parallel. In contrast to animals, a double fertilization event takes place in plants, producing two fertilization products, the embryo and the endosperm. Imprinting, the parent-of-origin–specific expression of genes, typically takes place in the mammalian placenta and in the plant endosperm. A prevailing hypothesis predicts that a parental tug-of-war on the allocation of available recourses to the developing progeny has led to the evolution of imprinting systems where genes expressed from the mother dampen growth whereas genes expressed from the father are growth enhancers. The number of imprinted genes identified in plants is low compared to mammals, and this precludes the elucidation of the epigenetic mechanisms responsible for this specialized expression system. Here, we have used genome-wide transcript profiling of endosperm without paternal contribution to identify seed regulators and, among these, imprinted genes. We identified a cluster of downregulated MADS-box transcription factors, including *AGL36*, that was subsequently shown to be imprinted by an epigenetic mechanism involving the DNA methylase MET1 and the glycosylase DME. In addition, the expression of the active *AGL36* allele was dampened by the FIS Polycomb Repressive Complex, identifying a novel mode of regulation of imprinted genes.

transferase MEDEA (MEA), FERTILIZATION INDEPENDENT SEED 2 (FIS2), FERTILIZATION INDEPENDENT ENDOSPERM (FIE), and MULTICOPY SUPPRESSOR OF IRA 1 (MSI1). The corresponding genes were identified in screens for autonomous endosperm development, indicating that the FIS complex acts as a repressor of endosperm development prior to fertilization [13–17].

An equally important regulatory mechanism in imprinting is DNA methylation resulting from the activity of several different methyltransferase enzymes, where each has specificity for cytosine (C) in certain sequence contexts. So far, imprinting has been shown to be under the influence of MET1, the major *Arabidopsis* maintenance DNA methyltransferase involved in CG-methylation [11,18–20]. DNA demethylation can be achieved either by a passive process i.e. the repression of *MET1* expression [21,22], or by an active mechanism involving DNA glycosylase enzymes such as DME [23]. Several lines of evidence show that DME, which is expressed in the central cell of the female gametophyte, is necessary for maternal-specific gene expression in the endosperm [11,18,19,24].

So far, only about a dozen genes in *Arabidopsis* have been identified to have parental-specific gene expression, and they illustrate different modes of imprinting [3]. *MEA, ARABIDOPSIS FORMIN HOMOLOGUE 5 (AtFH5)* and *PHERES 1 (PHE1)* are imprinted by the action of FIS PRC2, where only the latter is paternally expressed [13,25–31]. *FIS2, FLOWERING WAGENIN-GEN (FWA)* and *MATERNALLY EXPRESSED PAB C-TERMINAL (MPC)* are all maternally expressed and regulated by the dual action of MET1 and DME [11,19,24,32–34]. Recently, five novel imprinted genes, *HOMEODOMAIN GLABROUS 3 (HDG3), HDG8, HDG9, At5g62110* and *ATMYB3R2* were identified by differential DNA methylation in embryo and endosperm [35].

In comparison to *Arabidopsis*, more than 100 genes have been shown to have a uniparental or preferential parental expression pattern in mammals [36–39]. This suggests that additional genes in *Arabidopsis* are imprinted. Furthermore, the low number of

known imprinted genes in plants precludes the identification of general principles in this kind of gene expression control and thus, the identification of further imprinted genes is pivotal. Moreover, the targets of imprinted genes, as well as genomic pathways and regulatory modules influenced by imprinted genes are largely unknown.

Here, we have designed a microarray strategy for the identification of seed regulators by exploiting the *cdka;1* mutation. Using this approach, we have identified a cluster of previously uncharacterized AGAMOUS-LIKE (AGL) Type-I MADS-box transcription factors that are downregulated in endosperm with no paternal contribution. Here, we report that *AGL36* is imprinted by the dual action of MET1 and DME. In addition, *AGL36* is regulated throughout endosperm development in its maternal expression cycle by the Polycomb FIS-complex, thereby identifying a novel mode of regulation for imprinted genes.

Results

cdka;1 is a tool to identify key seed regulators

Here we have used *cdka;1* as a tool to identify factors sensitive to the vital parental gene balance in the endosperm. In heterozygous *cdka;1* mutants, the second pollen mitosis is either missing or is severely delayed. However, mutant pollen can successfully fertilize the egg cell while leaving the central cell unfertilized [40,41]. A detailed analysis by Aw and colleagues has revealed that a second sperm cell is delivered to the central cell, but that karyogamy does not take place [42]. Although not properly fertilized, the majority of the central cells in *cdka;1* fertilized ovules (70–90%) are triggered to initiate endosperm proliferation [40,42,43]. Thus, fertilization by *cdka;1* sperm cells creates a unique situation where endosperm initially develops without any paternal contribution (in the following also referred to as *cdka;1^P*). The endosperm, however remains under-developed, and ultimately the seed aborts, further demonstrating the importance of the paternal contribution to the endosperm for proper seed development. Since activation of maternal alleles by loss of maternal FIS PRC2 could rescue seed lethality [43], we hypothesized that the disturbance of parental gene balance in the endosperm is the main cause leading to developmental arrest of *cdka;1^P* at 3–4 days after pollination (DAP).

To identify factors and mechanisms sensitive to such an imbalance in gene dosage in the endosperm and with that likely key regulators of seed development, we performed microarray transcript profiling of *cdka;1* fertilized seeds at 3 DAP (Figure S1A). Due to the heterozygous nature of the *cdka;1* mutant line used, a transcript that is absent in *cdka;1^P* seeds will lead to a reduction of maximal 50% in the genome profiling experiment. For example, genes that are only expressed from the paternal genome would show such reduced expression levels (Figure S1B). Likewise, maternally expressed genes that require activation by a paternally expressed gene(s) would be downregulated (Figure S1C), whereas genes that are acted upon by paternally expressed repressors were expected to be upregulated in the microarray screen (Figure S1D).

When we compared the transcriptional profiles of Ler x *cdka;1* versus Ler x Col seeds 3 DAP, we detected 17223 nuclear genes that were expressed in all biological replicates of both mutant (*cdka;1* set) and wild-type (WT set) seed profiles. Our result is in good agreement with a set of genes identified by Goldberg & Harada laboratories (GH) in globular stage seeds of *Arabidopsis* Ws-0 plants as 68% of our genes were also identified by GH, and our gene set included >90% of the GH globular seed gene set (Figure 1A; http://seedgenenetwork.net, [44]).

To further validate the quality of our dataset, we examined the expression pattern of genes known to be preferentially expressed
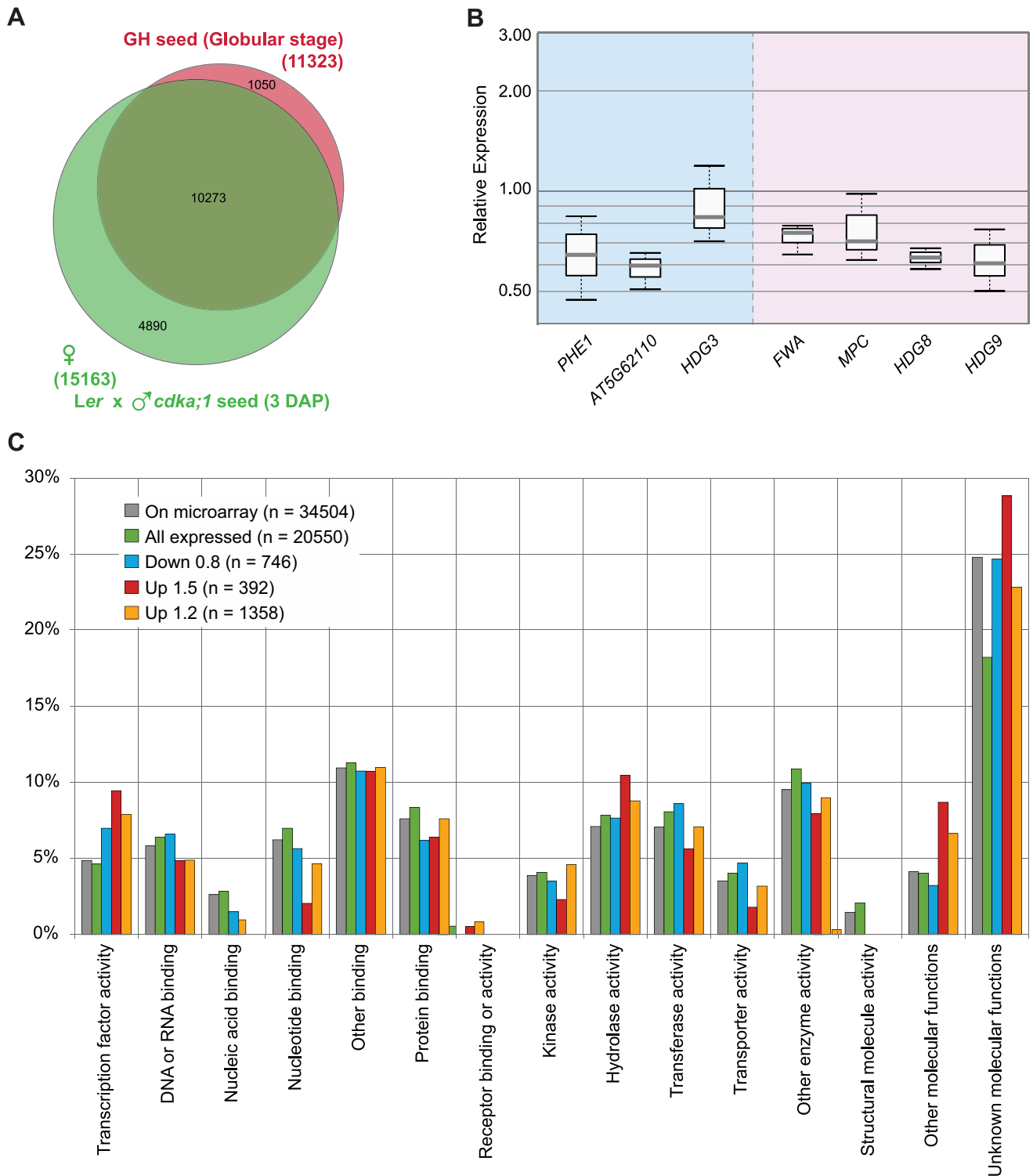
Figure 1. Analysis of *cdka;1* microarray profiles. (A) Venn diagram representing overlap of genes expressed in globular stage seeds of *Arabidopsis* Ws-0 plants (red) and genes expressed in 3 DAP seeds from L*er* plants pollinated with Col *cdka;1* pollen (green). As high as 67.8% of the *cdka;1* set and 90,7% of the GH set genes were found in the overlap. Gene numbers refer to the reference set of genes (see material and methods). GH: Goldberg & Harada laboratories (http://www.seedgenenetwork.net). (B) Boxplot showing the reduced relative expression of known maternally imprinted (blue background) and paternally imprinted (pink background) genes in the L*er* x *cdka;1* versus L*er* x Col seeds. Calculations are based on values taken from three independent biological replicas. (C) GO functional classification of microarray expression data. Deregulated genes identified in the microarray experiment were functionally classified regarding their molecular function using the GO Slim classification system (http://www. arabidopsis.org/tools/bulk/go/). The total number of unique GO-term:locus assignments for each group is indicated (n). The functional classifications of all genes present on the microarray (On microarray) and all genes having a present call (All expressed) have been included for comparison. The cut-off for deregulation is ≤0.8 for the downregulated group, and ≥1.5 and ≥1.2 for the upregulated groups.
doi:10.1371/journal.pgen.1001303.g001

from the paternal allele. To date, only three genes have been identified that show a predominant paternal expression pattern; *PHE1*, *HDG3* and *At5g62110*, where all three genes were found to be downregulated in our arrays (Figure S1E), supporting our working hypothesis that paternally expressed genes can be detected amongst downregulated genes. In addition, out of seven imprinted maternally expressed genes present in our microarray sets, four were also detected as downregulated (Figure S1E). This could reflect required activation by paternal factors (Figure S1C), or be a result of more complex deregulation in response to change in gene dosage. To exclude array artifacts we tested all down-regulated genes by means of real-time PCR and could confirm their deregulation (Figure 1B).

Due to the background noise in the microarray experiment, modest but reproducible downregulation of arithmetic ratios (ar) ranging from 0.5 to 1.0 will produce False Discovery Rates (FDR, see materials and methods) with insignificant *q* values. Since the absence of paternally expressed genes was the simplest hypothesis to account for downregulation, we defined a functional limit for screening purposes that allowed us to detect two out of three known paternally expressed genes in the array. Both *PHE1* and *HDG3* are detected at *q* values of 0.35 and a downregulation cutoff of 0.8 (ar). Consequently these values were chosen and used to filter the microarray data.

Using these criteria, a set of 602 genes was extracted (q≤0.35 and ar ≤0.8), subsequently called *Down 0.8*. For upregulation, we worked with two gene sets. For the first set, *Up 1.2*, we used parameters equivalent to the downregulated set (q≤0.35 and ar ≥1.2), which resulted in a set of 1030 genes. For the second set, *Up 1.5*, resulting in 323 genes, we chose ar ≥1.5, a threshold for deregulation commonly used in genome-wide expression studies (Table S3).

To test whether the deregulated genes could preferentially be attributed to a certain seed structure, we compared our data to gene sets expressed in different seed regions and compartments of globular stage seeds using data generated by Goldberg & Harada (GH) laboratories available at http://seedgenenetwork.net [44]. The overlap between the upregulated gene sets and the GH embryo, seed coat and endosperm was significantly lower than expected for independent sets of genes, indicating that among the upregulated genes we preferentially find those that are below the detection limit of the GH analyses. However looking at the downregulated genes, the picture was different. While we found slightly less overlap than expected by chance for the GH embryo set, the overlap was clearly larger than expected by chance for GH seed-coat ($1.2 < 2.7e^{-07}$) and even more significant for the GH endosperm (rf = 1.3, $p < 2.0e^{-13}$, Figure S2A, S2B).

Lack of the paternal genome results in the downregulation of a group of MADS-box Type-I Mγ transcription factors

In order to functionally classify the deregulated gene sets according to their molecular functions we used the GO Slim classification system (Figure 1C). Only for the GO Slim term "*Transcription factor activity*" we find a higher percentage and significant over-representation of both up- and down-regulated groups when compared to all genes on the array/all genes expressed. Since key regulators of seed development are likely to be transcription factors (TF), we analyzed this class in detail.

When comparing the fraction of deregulated genes among the different TF families, the Mγ MADS-box transcription factors clearly stood out with more than 60% of the seed expressed members being downregulated in Ler x *cdka;1* arrays (Figure S3A, S3B). We therefore focused on this MADS Type-I class for further

analysis. Searches in publically available expression databases (www.genevestigator.com, Figure S4) revealed that all identified genes were exclusively expressed in the seed and predominantly in the endosperm. From the identified Type-I Mγ MADS-box genes, we selected *AGL36* for further in depth analysis (Figure S4). *AGL36* was the previously undescribed Mγ candidate that interacted with the highest number of described AGLs in a Y2H screen performed by de Folter et al [45]. Both *AGL36* and *PHE1* have been shown to interact with AGL62, which plays a major role in endosperm development [45,46]. Within the Mγ class, *AGL36* clusters together with *AGL34* and *AGL90* [47], which are both also detected as downregulated in our microarray experiment (Figure S4). *AGL36* shares 85.7% and 84% nucleotide identity with *AGL34* and *AGL90*, respectively (Figure S8). On the amino acid level this results in of 80.2% similarity of AGL36 with AGL34 and 83.9% similarity with AGL90.

AGL36 is only expressed from its maternal allele

Real-time PCR measurement of *AGL36* relative expression level three days after pollination (3 DAP) in Ler ovules fertilized with either Col or *cdka;1* pollen confirmed that *AGL36* expression was reduced in *cdka;1* fertilized seeds, (27% when normalized towards *ACT11*, and 36% when normalized towards *GAPA*) compared to wild-type seeds (Figure 2A).

To determine whether *AGL36* has parental-specific expression, we took advantage of an *AGL36* Single Nucleotide Polymorphism (SNP) existing between the Col and Ler ecotypes. This SNP allows the PCR product of Col cDNA to be digested by *Alw*NI, leaving the Ler cDNA PCR product intact (Figure 2B). We performed reciprocal crosses between Col and Ler ecotypes, and analyzed the digested RT-PCR fragments on an Agilent Bioanalyzer Lab-on-a-Chip, allowing accurate measurement of fragment sizes and their concentrations. When Col[maternal] is crossed with Ler[paternal], we only detected the Col bands (165 bp+234 bp) after *Alw*NI digestion, indicating only maternal expression (Figure 2C). Similarly, in the reciprocal cross when Ler[maternal] is fertilized with Col[paternal] pollen, the cDNA PCR digest resulted only in an undigested band (399 bp) originating from Ler, indicative of maternal expression (Figure 2C). This testified that *AGL36* was only expressed from the maternal genome after fertilization and thus identified as a novel imprinted gene.

AGL36 is imprinted throughout early seed development

AGL36 expression level in wild-type seeds (Ler x Col) at different stages of seed development was monitored over a period of 12 days after pollination. Initially, a low expression level was detected (1 DAP), followed by a rapid increase and subsequent peak in *AGL36* expression at 4 DAP, when the embryo is at the late globular stage of development, before declining (Figure 3A). At the embryo heart stage, corresponding to 6 DAP, *AGL36* expression had decreased to similar levels as 1 DAP. To address whether *AGL36* imprinting is maintained throughout its expression cycle, we performed a SNP analysis of the RT-PCR product obtained from Ler x Col crosses harvested during 1 to 12 DAP (Figure 3B). We found that *AGL36* expression is originating from the maternal genome (Ler) throughout the experiment. By plotting the molarities of the maternal band obtained by Agilent Bioanalyzer, an expression profile closely identical to the pattern obtained in the real-time PCR analysis was found (Figure 3C).

To rule out that the observed maternal expression is due to expression of *AGL36* in the ovule integument, which is a maternal tissue, we generated a reporter construct consisting of 1752 bp of the *AGL36* promoter region fused to a *GUS* reporter (*pAGL36::-GUS*) (Figure 4A). Single-copy lines carrying this construct were
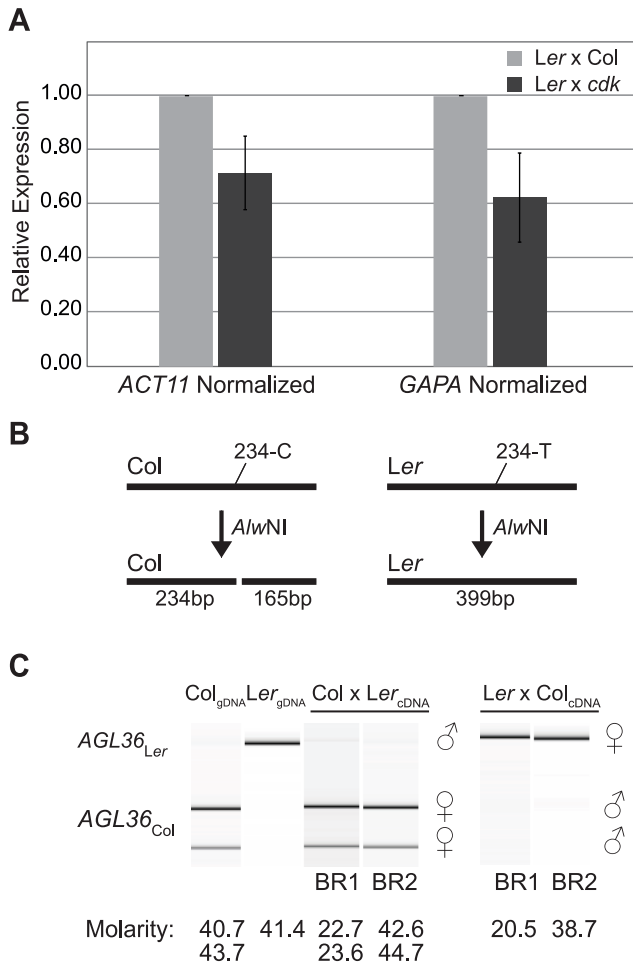
A

B

C

Molarity: 40.7 41.4 22.7 42.6   20.5 38.7
43.7   23.6 44.7

Figure 2. AGL36 is only expressed from the maternal genome.
(A) Real-time PCR analysis showing *AGL36* expression in L*er* x *cdka;1* relative to L*er* x Col seeds 3 DAP. Gray bars represent L*er* x Col expression levels, black bars represent the L*er* x *cdka;1* expression levels. Left section: *AGL36* normalized to *ACT11* levels. Right section: *AGL36* normalized to *GAPA* levels. Average values from three independent biological replicas are shown. Error bars indicate standard deviation (STDEV). (B) Schematic overview of *AGL36* SNP analysis. The presence of a SNP between Col and L*er* ecotypes (C-T conversion respectively) allows the amplified *AGL36* cDNA PCR product from the Col ecotype to be digested with *Alw*NI restriction enzyme, while the L*er* ecotype remains undigested. (C) *AGL36* is maternally expressed. Seeds obtained from Col x L*er* and L*er* x Col crosses were harvested at 3 DAP followed by *AGL36* RT-PCR, *Alw*NI digestion and subsequent Bioanalyzer analysis. Genomic Col and L*er* were included as controls (Left section, first two lanes). Digestion products of two independent biological replicas of maternal Col x L*er* pollen crosses produced only Col bands, indicating maternal expression (Middle section). Similarly, the digestion products of two independent biological replicas of maternal L*er* x Col pollen produced only L*er* bands, indicating maternal expression (Left section). The intensities of the bands are represented as concentrations (nmol/L), and create a basis for comparison. 100 ng DNA was used as template for each PCR reaction.
doi:10.1371/journal.pgen.1001303.g002

used in reciprocal crosses with wild-type L*er* and Col plants to examine *GUS* expression at 3 and 6 DAP. When inherited maternally, *pAGL36::GUS* expression in the seed was indeed found to be restricted only to the fertilization product (Figure 4B, Figure S7D). In the reciprocal cross, when *pAGL36::GUS* was inherited from the paternal genome, no *GUS* expression was detected, (Figure 4C, Figure S7E). Consistent with the SNP analysis, this
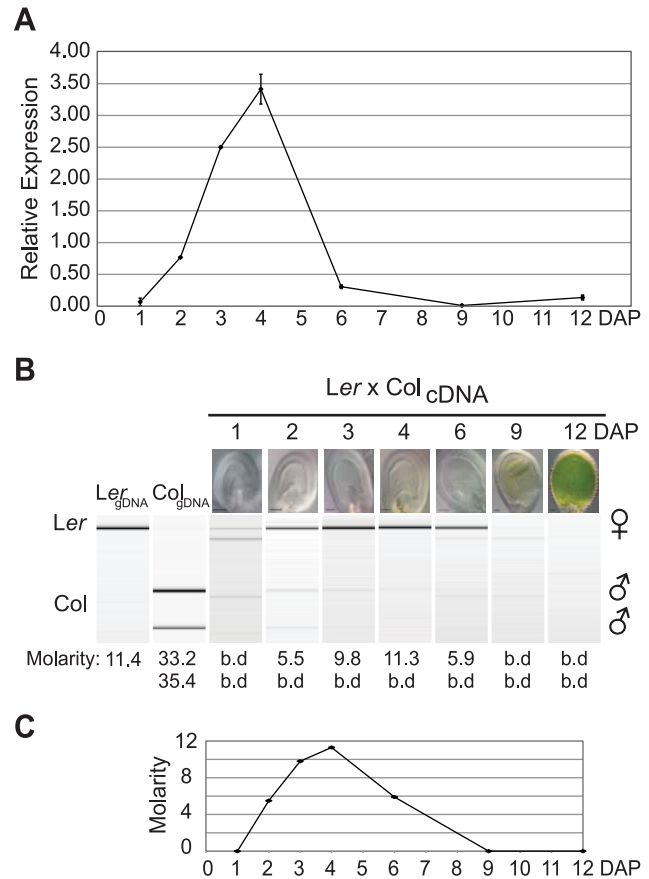
A

B

Molarity: 11.4 33.2 b.d 5.5 9.8 11.3 5.9 b.d b.d
35.4 b.d b.d b.d b.d b.d b.d b.d

C

Figure 3. AGL36 is imprinted throughout its expression cycle.
(A) *AGL36* expression profile. Calculations were done using 3 DAP values as reference point, giving other obtained expression values relative to the 3 DAP expression level. Samples were taken at 1, 2, 3, 4, 6, 9, and 12 DAP. The graph represents the average relative expression values obtained from two independent biological parallels where the RNA from each biological sample gave rise to two independent cDNA syntheses (technical replica). The indicated STDEV is derived from the two independent biological parallels. The *AGL36* transcript levels were normalized to *ACT11* levels. (B) RT-PCR digest of the SNP containing region analyzed by the Bioanalyzer show that *AGL36* imprinting is maintained throughout seed development. Samples were taken at time-points as indicated for each lane. A representative light micrograph of each DAP stage is shown. Only maternal (L*er*) *AGL36* expression was found when present. Genomic L*er* and Col DNA were included as controls. 100 ng DNA/cDNA was used as template for each PCR reaction. The intensities of the bands are represented as concentrations (nmol/L). Note, weak paternal bands obtained at 2 DAP were below the detection limit for measurement on our instrument (0.1 ng/μl~0.4 nmol/L). Intensities below the detection point of the instrument are indicated as b.d. The displayed SNP picture is representing one of four independent runs (2BR and 2TR). (C) Visual representation of the obtained intensities of maternal bands in B) represented as concentrations (nmol/L).
doi:10.1371/journal.pgen.1001303.g003

demonstrated that *AGL36* was imprinted and only maternally active throughout its expression cycle. Furthermore, the 1.7 Kb promoter fragment used in this analysis appears to be sufficient to confer parent-of-origin specific expression of the reporter.

AGL36 is not required for seed survival

To further investigate the biological function of *AGL36*, we screened the Koncz T-DNA collection for insertions [48]. We identified a mutant line, *agl36-1*, harboring a single T-DNA
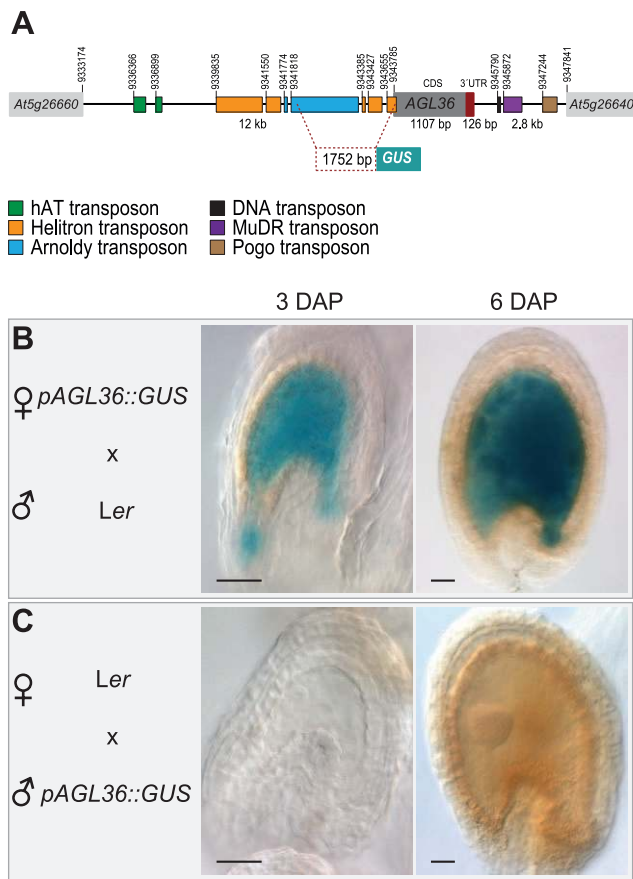
Figure 4. pAGL36::GUS is expressed only from its maternal allele (and only in the fertilization products). (A) A pAGL36::GUS construct was generated using 1752 bp of the promoter region of AGL36 that spans the ATG start codon. Transposable element sequences (hAT, Helitron, Arnoldy, DNA transposons, MuDR and Pogo transposons) in 5′ and 3′ regulatory regions are color coded as indicated. The numbers indicate the positions on Chromosome 5 (http://gbrowse. arabidopsis.org). Note, Helitron and Arnoldy transposable elements in the pAGL36::GUS promoter region. Plants expressing the transgene were used either as maternal (B) or paternal (C) partners in crosses with wild-type plants. Samples were taken at 3 DAP (left panel) and 6 DAP (right panel). pAGL36::GUS is absent in the seed-coat and only maternally expressed in the endosperm. The pAGL36::GUS signal is increased in 6 DAP versus 3 DAP samples.
doi:10.1371/journal.pgen.1001303.g004

insertion 16 bp upstream of the AGL36 ATG start codon (Figure S5A). The agl36-1 line showed Mendelian segregation of the T-DNA insertion, as 75% of the plants were resistant to Hygromycin (N = 1025, $\chi^2 = 0,83$, Table S1).

To test the transmission through the male and female gametes directly, reciprocal crosses of both hemizygous and homozygous agl36-1 mutant plants with wild-type plants were performed (Table S1). In a reciprocal cross, a hemizygous mutant will segregate 50% of the T-DNA resistance marker if the disrupted gene is not vital for gametophyte transmission or function. Thus, gametophyte requirement can be scored directly as reduced frequency of resistant plants [49]. In reciprocal crosses with agl36-1, no transmission distortion through female or male gametophytes could be observed (N = 661, $\chi^2 = 0,13$ and N = 1015, $\chi^2 = 0,00$ respectively, Table S1).

The position of the T-DNA insertion in agl36-1 predicts AGL36 expression failure, and indeed real-time PCR analyses of 3 DAP

seeds of homozygous agl36-1$^{-/-}$ plants compared to Col wild-type indicate a 1000-fold AGL36 downregulation in the mutant seeds (Figure S5B). In line with an imprinted and maternal-only expression of AGL36, close to 50% reduction of the transcript level was observed in 3 DAP hemizygous agl36-1$^{+/-}$ seeds (Figure S5B). We thereby concluded that agl36-1 represents a loss-of-function allele of AGL36.

Although depletion of AGL36 did not interfere with the fitness of the mutant allele in our experimental system, we have shown that AGL36 is specifically expressed from the maternal allele in the fertilization product, in a time frame between 2 and 6 DAP. To investigate whether this was reflected morphologically or developmentally in the developing seed, we compared embryo and endosperm development in wild-type and homozygous agl36-1$^{-/-}$ seeds within the AGL36 expression time frame.

After fertilization of the egg and the central cell, the endosperm in Arabidopsis undergoes three syncytial rounds of nuclear divisions before the first asymmetric division of the zygote that creates the apical embryo proper and the basal suspensor that connects the embryo proper and the maternal tissue (Figure S5C). At the 2 DAP stage, no obvious difference could be observed between wild-type and agl36-1$^{-/-}$ seeds, both typically harboring a 1–2 cell embryo proper and a 16–32 nucleated endosperm (Figure S5C, left section). The embryo continues to divide through radial, longitudinal and transverse divisions to produce the so-called globular stage at 4 DAP (Figure S5C, middle section). The endosperm also undergoes 3–4 syncytial nuclear divisions and remains uncellularized as cell proliferation at the upper half of the embryo forms the cotyledon primordia at the so-called heart stage at 6 DAP (Figure S5C, right section). Although the main AGL36 expression peak occurs during this time frame, no obvious deviation between wild-type and agl36-1$^{-/-}$ could be observed at these stages. Similarly, using an endosperm specific pFIS2::GUS reporter [33], a wild-type endosperm division pattern was observed in agl36-1$^{+/-}$ seeds (Figure S5D).

MET1 is required for AGL36 imprinting

The majority of imprinted, maternally expressed genes identified in Arabidopsis so far have been shown to be paternally silenced by mechanisms involving symmetric CG methylation, maintained by MET1 [11,18,19]. Although not directly linked to imprinting, methylation can also be directed by CHROMO-METHYLASE 3 (CMT3) that has specificity for CNG, and members of the DOMAINS REARRANGED METHYL-TRANSFERASE (DRM) family; DRM1 and DRM2, that are mainly responsible for asymmetric CHH methylation [50]. In order to address the involvement of DNA methylation in the regulation of paternal AGL36 expression, we performed SNP analyses of 3 DAP ovules from reciprocal crosses with mutants that have been shown to be involved in DNA methylation. In the SNP RT-PCR analysis of mutant pollen crossed to wild-type, paternal AGL36 expression is expected if the tested mutants are involved in AGL36 imprinting.

CMT3 DNA methylation has been reported to be guided to specific sites by KRYPTONITE (KYP) H3K9 methylation [51]. When mutant cmt3-7 and kyp-2 pollen were crossed to Col wild-type plants, no difference in AGL36 expression was observed (Figure 5A). In the reciprocal cross with cmt3-7 also no difference could be detected compared to wild-type expression (Figure S6).

DRM1 and DRM2 are mainly responsible for asymmetric DNA CHH methylation [50] and rely on small interfering RNAs, processed by ARGONAUTE4 (AGO4), for target template guidance [52]. In our assays, fertilization by pollen lacking DRM1;DRM2 and pollen lacking AGO4 had no effect on the
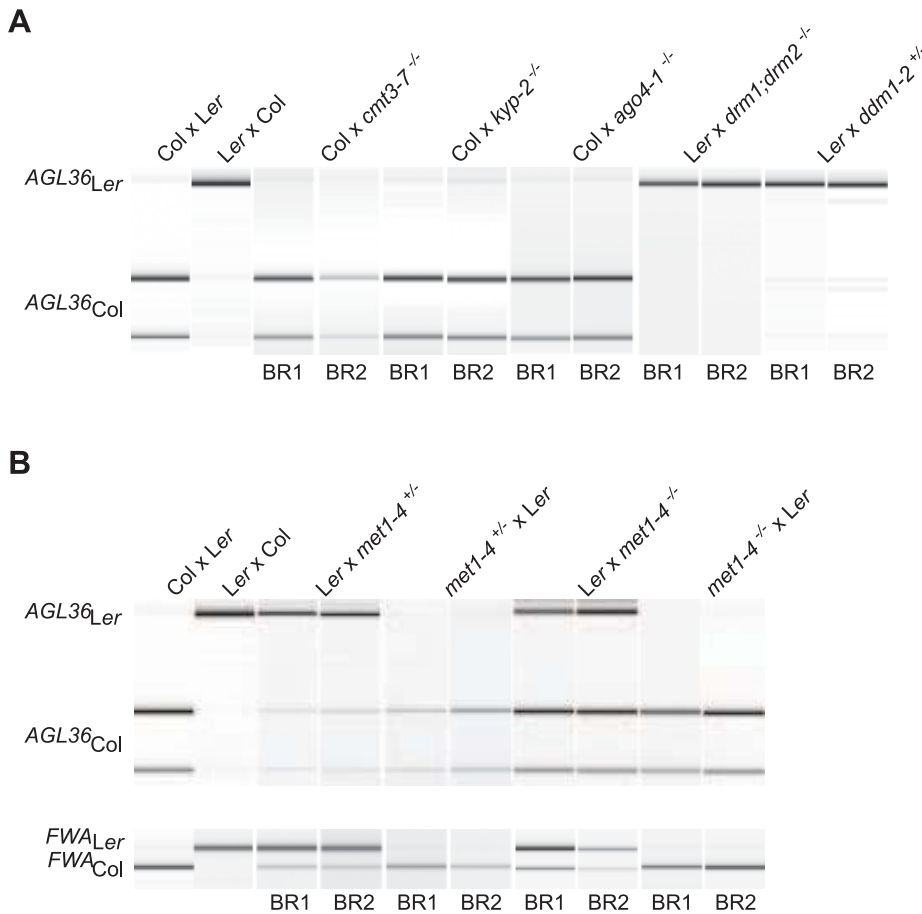
Figure 5. The effect of DNA methylation on parental AGL36 expression. (A,B) SNP analyses of 3 DAP seeds from crosses with DNA methylation mutants. The amplified SNP containing regions of AGL36 and FWA cDNA were digested with AlwNI and NheI, respectively, and analyzed in a Bioanalyzer. (A) Homozygous cmt3-7, kyp-2, and ago4-1 mutants in the Ler ecotype were used as pollen donors to pollinate Col plants, while homozygous drm1;drm2 and heterozygous ddm1-2 mutants in the Ws-2 and Col ecotype respectively, were used as male to fertilize Ler ovules. No paternal AGL36 expression could be detected in these crosses. (B) Upper panel: Hemizygous met1-4$^{+/-}$ in the Col ecotype reciprocally crossed with Ler wild-type plants show that the paternal allele of AGL36 is expressed when met1-4 is crossed as male. No paternal bands are observed when met1-4 is used as the maternal cross partner. Using pollen from first generation met1-4$^{-/-}$ homozygous plants in a Ler x met1-4$^{-/-}$ cross gives rise to prominent bands of the digested paternal Col expression product. In the reciprocal met1-4$^{-/-}$ x Ler cross no paternal expression can be detected. Lower panel: FWA control using the same tissue as above showing imprinted expression of FWA in dependence of MET1. Paternal FWA expression was observed when plants hemizygous and homozygous for met1-4 were crossed as male to Ler wild-type.
doi:10.1371/journal.pgen.1001303.g005

AGL36 expression pattern (Figure 5A). Likewise, AGL36 expression in the reciprocal cross was identical to wild-type (Figure S6).

DECREASE IN DNA METHYLATION1 (DDM1) is involved in maintenance of DNA methylation [53]. In our SNP RT-PCR analyses where mutant ddm1-2 pollen was used to fertilize wild-type ovules, paternal AGL36 expression was not activated (Figure 5A). In summary, CMT3, KYP, DRM1;DRM2, AGO4 and DDM1 appear not to be involved in the establishment nor maintenance of AGL36 imprinting (Figure 5A, Figure S6).

However, paternal AGL36 expression was detected when plants hemizygous for the met1-4 mutation were used as pollen donor in crosses with wild-type Ler (Figure 5B). In the reciprocal cross, using met1$^{+/-}$ as the maternal partner, no AGL36 expression from the paternal genome could be observed (Figure 5B). Furthermore, we performed crosses using pollen from homozygous met1-4 parents. When first generation homozygous met1 plants were used as pollen donor on wild-type plants, prominent AGL36 expression from the paternal Col genome could be observed (Figure 5B). This strongly suggests that the repression of the paternal copy of AGL36 is lifted due to the met1-4 mutation, and that MET1 is required for

maintaining paternal inactivation of AGL36. In the reciprocal crosses, only expression from the maternal genome could be detected, both in the heterozygous and the homozygous met1-4 situation, further substantiating the requirement of MET1 in the male germline in order to maintain AGL36 imprinting (Figure 5B). Maternal AGL36 expression levels using homozygous met1-4 as the maternal cross partner appeared to be equal to maternal levels in the reciprocal crosses (Figure 5B). This opens for the interpretation that DNA methylation is not required for the regulation of maternal AGL36 expression.

Silencing of vegetative AGL36 expression involves MET1

In public expression databases, AGL36 is reported to be expressed in the seed and more precisely in the endosperm [54] (Figure S4). In order to monitor AGL36 expression in vegetative tissues and its dependence on DNA methylation, we performed a real-time PCR experiment on vegetative tissues from reciprocal Ler x Col crosses and homozygous met1-4 tissues. In biological replicates of progenies from both reciprocal crosses, weak AGL36 expression ranging from 1–6% of the seed expression level could

be detected in seedlings, leaves and flowers (Figure 6A). This showed that *AGL36* was expressed throughout the plant life cycle, although at very low levels. In the same experiment, we monitored expression in *met1-4* tissues. *AGL36* expression levels were 50–90-fold higher in *met1-4* leaves compared to seed expression levels (Figure 6A). In a direct comparison, expression levels were elevated 2000-fold in homozygous *met1-4* leaves compared to wild-type Col x L*er* leaves (Figure 6B). In flowers, the upregulation was more than 20-fold in *met1-4* compared to wild-type Col x L*er* flowers (Figure 6C). In conclusion, these data showed that silencing of *AGL36* in vegetative tissues involves MET1, suggesting that the absence of maintenance DNA methylation elevates vegetative *AGL36* expression beyond the maternal expression levels found in seeds.
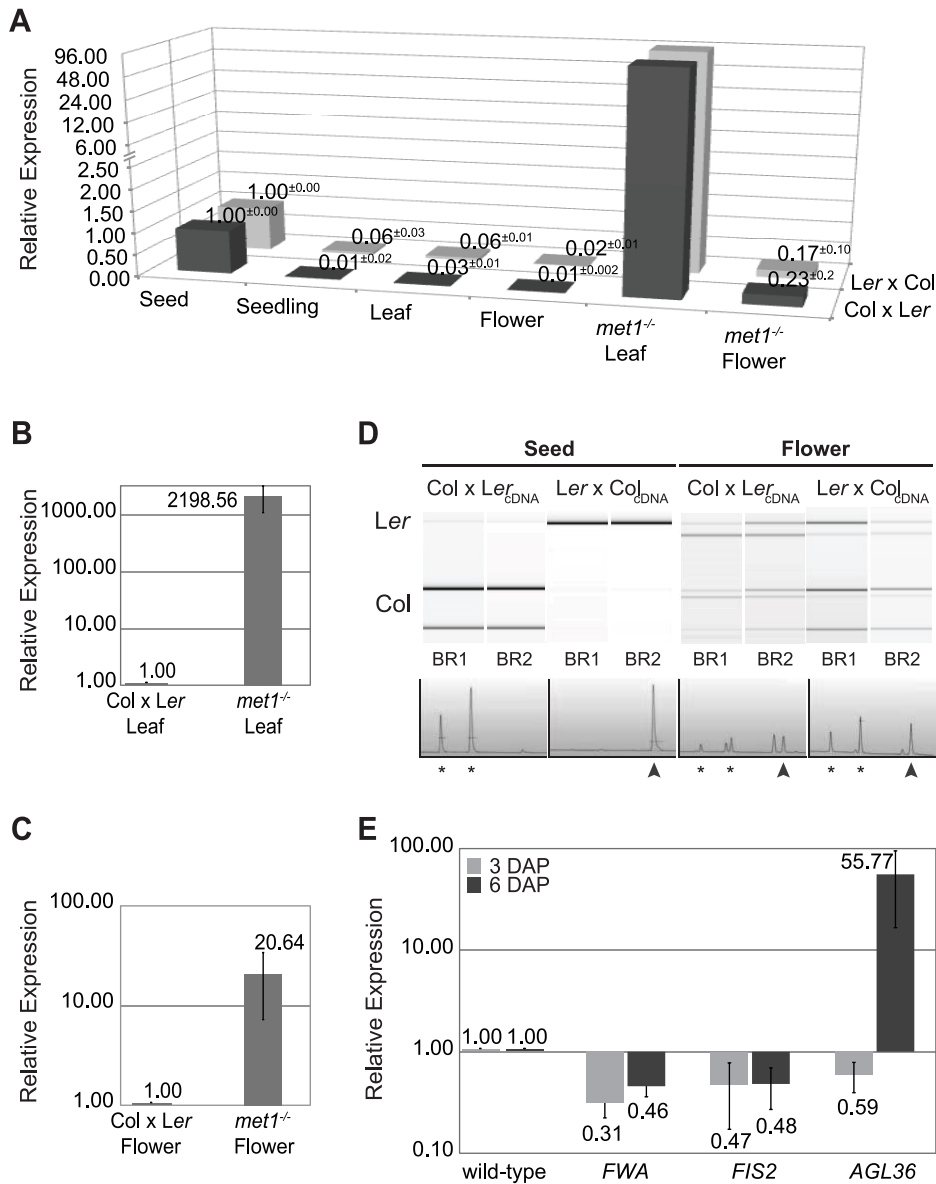

Figure 6. *AGL36* expression is controlled by MET1 and DME. (A) Real-time PCR of *AGL36* expression levels in seeds, seedlings, leaves and flowers in F1 progenies of L*er* x Col (gray bars), and Col x L*er* (black bars) plants. *AGL36* expression level in leaves and flowers of *met1*$^{-/-}$ selfed plants in the Col ecotype are shown in the two rightmost bars. All expression levels shown are relative to the *AGL36* expression levels in 3 DAP seeds. (B–C) Expression levels of *AGL36* in leaves (B) and flowers (C) of *met1*$^{-/-}$ plants (Col) relative to expression level in F1 progenies of Col x L*er* plants. (A–C) represent the average relative expression values obtained from two independent biological parallels (BR) where each gave rise to four independent cDNA syntheses (TR). STDEV is derived from the two BRs. *ACT11* is the reference gene used. (D) Parental dependence of *AGL36* expression in seeds and flowers. SNP analyses of 3 DAP seeds (left) and F1 hybrid flowers (right) obtained from Col x L*er* and L*er* x Col crosses. The amplified SNP containing region of *AGL36* was *Alw*NI digested and analyzed in a Bioanalyzer. Seeds express *AGL36* only from the maternal genome (left). Flowers express *AGL36* biparentally (Note both L*er* and Col bands (right)). The electropherograms represent one BR. Peaks are representing the bands shown in the graph. Asterisk; digested Col product, Arrowhead; undigested L*er* product. (E) Real-time PCR expression levels of *FWA*, *FIS2* and *AGL36* in *dme-6* x Col vs. wild-type seeds 3 and 6 DAP. Graphs represent the average relative expression from four independent BRs. Values for *FIS2* are calculated based on 3 BRs as the value for the fourth BR was clearly out of range. Samples used in the first BR gave rise to two TRs. STDEV is derived from the independent BRs. *ACT11* is the reference gene used.
doi:10.1371/journal.pgen.1001303.g006

AGL36 is biparentally expressed in vegetative tissues

In order to investigate the parental expression pattern of *AGL36* in vegetative tissues, we performed SNP analyses of flowers from F1 hybrids of L*er* and Col reciprocal crosses. In both reciprocal crosses, *AGL36* appeared to be expressed equally from the parental L*er* and Col genomes, indicating biparental expression in flowers (Figure 6D). This indicates that parental-specific expression, i.e. imprinting of *AGL36*, as expected, only takes place in the seed and that a low basal biparental expression is present throughout the plant life cycle. Interestingly, biallelic expression in flowers suggests that further silencing of *AGL36* takes place in the male germline before uniparental expression in the seed (Figure 6D).

AGL36 is controlled by DEMETER

According to our data, the action of MET1 suppresses *AGL36* expression throughout the vegetative phase and this suppression is maintained in the fertilization product through the male germline. *AGL36* imprinting thus requires specific activation of the maternal allele. DNA demethylation by DME has previously been shown to mediate maternal-specific gene expression in the endosperm [11,18,19,24], and we therefore investigated *AGL36* expression in *dme-6* mutant plants. Since *dme* cannot be maintained in a homozygous state, we harvested siliques of $dme-6^{+/-}$ heterozygous plants pollinated with Col pollen at 3 and 6 DAP. We monitored the relative expression by means of real-time PCR using *FWA* and *FIS2* as controls. At 3 DAP, both controls were downregulated by $69^{\pm0.09}\%$ and $53^{\pm0.30}\%$ respectively (Figure 6E), in line with a lack of functional DME in 50% of the seeds in heterozygous $dme-6^{+/-}$ plants. *AGL36* was downregulated in a similar manner as *FIS2* $(41^{\pm0.20}\%)$, suggesting that DME is indeed involved in early activation of the maternal *AGL36* allele.

Expression of maternal AGL36 is regulated by the PRC2 FIS-complex

We also tested the expression of *FWA* and *FIS2* in 6 DAP samples and found that their downregulation were sustained as predicted (Figure 6E). However, to our surprise *AGL36* expression in $dme-6^{+/-}$ seeds was elevated more than 50-fold (Figure 6E). This result was unexpected, and implicated a more intricate regulation of *AGL36*.

DME is required for the activation of *MEA*, the core histone H3K27 methyltransferase (HMTase) of the PRC2 FIS-complex [46,55,56]. To determine whether PRC2 FIS is involved in the regulation of *AGL36*, we analyzed the relative expression of *AGL36* over time (1 to 12 DAP) in *mea* mutant seeds compared to wild-type (Figure 7A). While *AGL36* expression in wild-type seeds was at its maximum at 4 DAP, we observed that *AGL36* expression in *mea* seeds surpassed the maximum levels of wild-type at 4 DAP, and reached its highest levels at around 6 DAP. At this point, the *AGL36* relative expression in *mea* mutant seeds was approximately 40-fold higher than wild-type expression at the same stage, and 7-fold higher than the maximum *AGL36* level found in wild-type seeds at 4 DAP (Figure 7A). Our data thus indicate that the FIS-complex is indeed a repressor of *AGL36* expression, and could also explain the elevated *AGL36* expression level in 3 DAP $dme-6^{+/-}$ seeds (Figure 6E). In line with these findings, we found highly elevated *AGL36* relative expression levels in mutant seeds from three different mutant alleles of *mea* (Figure 7C). Similar results were also obtained with mutants of other components of the FIS PRC2 complex (FIS2, FIE and MSI1, data not shown).

To investigate whether FIS activity was exerted on the maternal and/or paternal allele of *AGL36*, we performed SNP analyses on the RT-PCR product of *AGL36* obtained from *mea* mutant plants

(in L*er* background) pollinated with Col wild-type pollen. We found that *AGL36* is expressed only from its maternal allele in the *mea* background throughout the duration of our experiment (Figure 7B). In comparison to the expression pattern in wild-type (Figure 3B), strong ectopic maternal expression was also observed at 9 and 12 DAP stages. No paternal expression could be observed in these stages. By plotting the molarities of the maternal band detected by the Agilent Bioanalyzer, an expression profile for the maternal allele could be generated (Figure 7B, lower panel). This demonstrated that in the absence of MEA, *AGL36* expression continues to increase after 4 DAP, and although the intensity decreases from 6 DAP, high level of *AGL36* is maintained at 12 DAP. Hence, the FIS-complex represses the maternal allele of *AGL36* after the 3 DAP stage.

To further substantiate that maternal *AGL36* expression is regulated by the maternal action of MEA, we crossed *mea* mutant plants with pollen expressing the *pAGL36::GUS* reporter line. Here, no obvious activation of the paternal transgene could be observed at 3 DAP (Figure S7A). Surprisingly, at 6 DAP, corresponding to embryo heart stage, weak expression of the paternal copy in the embryo could be found (Figure S7A). In addition, we performed reciprocal crosses with the *pAGL36::GUS* reporter line in mutant *mea* background. When the transgene was contributed from the female side in *mea* background, a GUS signal was found in 3 DAP stages that increased drastically up to 6 DAP (Figure S7B). In the reciprocal cross however, no expression could be observed (Figure S7C).

The E(z) class of H3K27 histone methyltransferases (HMTases) in *Arabidopsis* consists of MEA, SWINGER (SWN) and CURLY LEAF (CLF) that participate in different PRC2 complexes. To test whether *AGL36* repression is a specific function of FIS^MEA PRC2, we analyzed *AGL36* expression in homozygous *swn-4* and *clf-2* seeds. For mutants of both HMTases values similar to the wild-type situation were found, and in conclusion *AGL36* appear to be specifically regulated by FIS^MEA PRC2 (Figure 7C).

In summary, maternal *AGL36* expression appears to be repressed specifically by the maternal action of FIS PRC2.

PRC2 acts on a subset of MET1/DME–regulated genes

For all genes known to be imprinted by PRC2, the FIS-complex is involved in the repression of the silenced allele [25-27,30,56]. Our data suggest that silencing of the paternal *AGL36* allele requires MET1 whereas the maternal allele is activated by DME. Modulation of female *AGL36* expression by PRC2 thus represents a novel mechanism in this type of gene expression system, and adds an additional level of parent-of-origin specific gene expression to the scheme. In order to investigate if this regulation applies to other genes imprinted by the dual action of MET1/DME [11,18,19], we analyzed the relative expression levels of *FWA*, *FIS2*, *AGL36* and *MPC* in a *mea* mutant. At 3 DAP expression levels were unchanged or slightly downregulated (0.40–0.99) for all genes tested (Figure 7D). However, while the expression of *FWA* and *FIS2* remained stable at 6 DAP, *AGL36* and *MPC* levels were elevated up to 80-fold (Figure 7D). Thus, genes imprinted by means of MET1/DME can be divided in two classes based on their dependence of FIS PRC2 for additional regulation of the expressed allele. Whereas one class appears not to be regulated by FIS PRC2, the other class depends on the action of the FIS-complex for developmental regulation of its expression.

Discussion

We have performed genome-wide microarray transcript profiling of seeds with only maternal endosperm as a screening
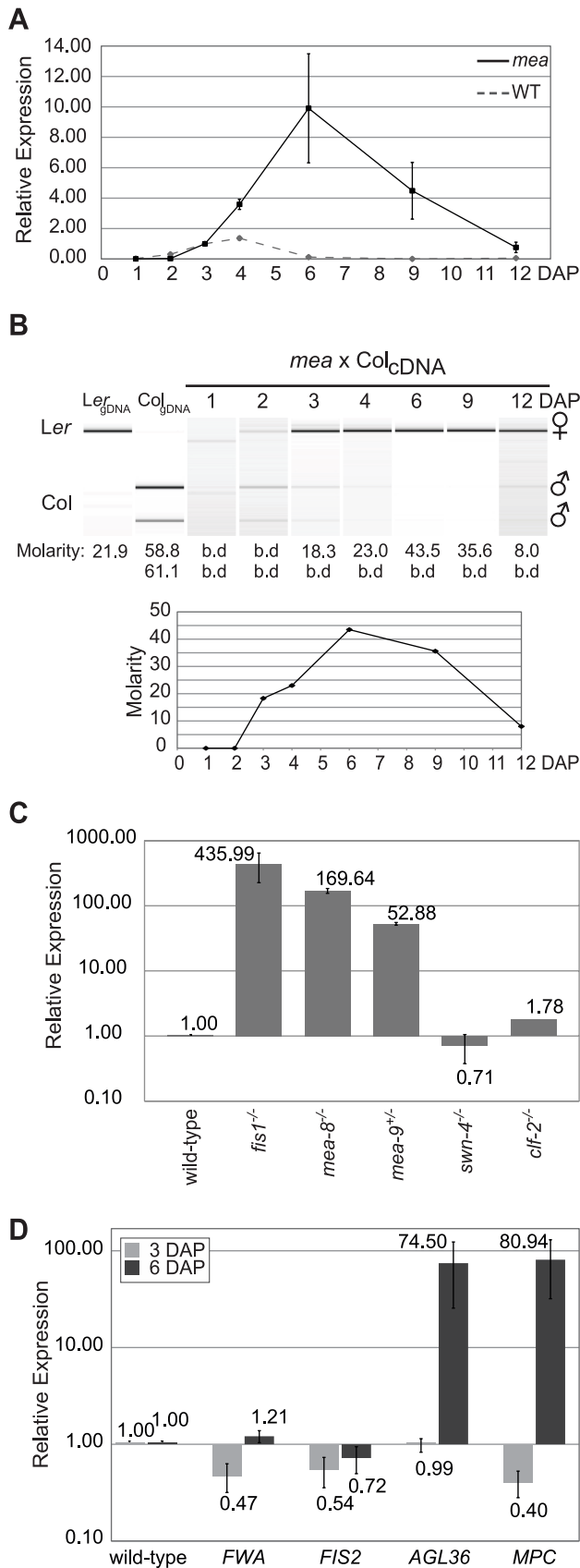
Figure 7. The maternal AGL36 allele is regulated by the PRC2 FIS-complex. (A) Real-time PCR AGL36 expression profile in 1–12 DAP wild-type and mea mutant seeds. 3 DAP values were used as the reference point for calculations. Samples were taken at indicated time points. The graph represents average expression obtained from two BRs and subsequent two TRs. STDEVs are derived from biological parallels. ACT11 is the reference gene used. (B) The FIS-complex regulates the maternal allele of AGL36. The PCR product of AGL36 SNP region obtained from mea x Col fertilized seeds was AlwNI digested and analyzed. Genomic Ler and Col DNA were included as controls. The intensities of the represented bands (nmol/L), allows comparison between different time-points. Note, unsustainable weak paternal signals at 2 and 3 DAP are below the detection limit for measurement on our instrument (0.1 ng/μl~0.4 nmol/L) and indicated as b.d. The chart represents the obtained concentrations from each sample. The displayed SNP picture is representing one of four different runs (2BRs and 2TRs). (C) AGL36 is regulated in three different alleles of mea but not in the E(z) MEA paralogues, clf and swn. Real-time PCR analysis showing AGL36 expression in (mea) fis1$^{-/-}$, mea-8$^{-/-}$, mea-9$^{+/-}$, swn-4$^{+/-}$ and clf-2$^{-/-}$ compared to wild-type. STDEVs are derived from two independent BRs. ACT11 is the reference gene used. (D) Real-time PCR expression level of FWA, FIS2, AGL36 and MPC in mea-9 x Col vs. wild-type seeds 3 and 6 DAP. Graphs represent the average relative expression values obtained from four independent BRs. Samples used in the first biological parallel gave rise to two TRs. STDEVs are derived from the independent BRs. The transcript levels were normalized to ACT11 levels.

doi:10.1371/journal.pgen.1001303.g007

method to identify novel regulators of seed development. Previous experiments have shown that a paternal genomic contribution is essential in wild-type *Arabidopsis* plants for successful seed development. Thus, our working hypothesis was that in the absence of the paternal genome in the endosperm, key regulators of seed development are not present or not effectively transcribed.

Using selection criteria that allowed for the identification of known paternally expressed genes, we extracted a set of downregulated genes that significantly overlapped with a set of endosperm expressed genes identified by Goldberg & Harada laboratories. The GO-Slim term *Transcription factor activity* was overrepresented in both down- and up-regulated gene sets, and a closer analysis revealed a striking overrepresentation of the Type-I Mγ MADS-box class among the downregulated transcription factors. With the selection criteria used, each detected gene could be a false positive at a probability of 0.35 at the highest, and thus a thorough examination of candidate genes, as performed in this report for *AGL36*, will be required.

MADS-box transcription factors play important roles in developmental control and signal transduction pathways in most if not all eukaryotes [57]. They are divided into two groups: the very well studied Type-II group (46 genes) including the MIKC class with important regulators such as AGAMOUS, and the Type-I group (61 genes), on which there is very limited information related to function [54,58,59]. Emerging data suggest that Type-I MADS-box genes differ from Type-II genes by being involved in female gametophyte and seed development [46,60–62]. In addition they were found to be only weakly expressed, and most members of this group contain no introns [63].

A comprehensive interaction study with members of the *Arabidopsis* MADS-box protein family by de Folter and colleagues indicated a complex network of interactions between these proteins (Figure S4). It revealed for instance that PHE1 interacts with AGL62, which in turn interacts with both AGL36 and AGL80. *AGL62* itself is regulated by the FIS-complex, and functions as a suppressor of endosperm cellularization [46,59]. PHE1 and AGL36 on the other hand both interact with AGL28. In addition, mutant analysis has shown that AGL80 function is

required for the expression of *DME* in the central cell, and is therefore an upstream regulator of FIS PRC2 [60]. Moreover, AGL61 is required for central cell development, and there is evidence that a heterodimerization between AGL61 and AGL80 is necessary for AGL61 translocation to the nucleus [59,62]. *PHE1* expression is upregulated in *A. thaliana* (*At*) x *A. arenosa* (*Aa*) incompatible hybrids due to loss of maternal *PHE1* silencing, and introgression of *phe1* could improve seed viability in semi-compatible 4x*At* x 2x*Aa* crosses [64]. In *A. thaliana*, expression of a *PHE1* antisense construct (*MEApromoter::asPHE1*) could partially restore the seed abortion phenotype in *mea* mutants [29]. Peculiarly, *PHE1* loss-of-function has no phenotypic effect in *A. thaliana* [56]. However, given the high sequence similarity within the Mγ class of Type-I MADS-box factors, it is possible that *MEApromoter::asPHE1* silenced not only *PHE1* but also many other Mγ class genes. Taken together, it seems likely that additional Type-I MADS-box factors are upregulated in *mea* mutants and a collective downregulation by antisense *PHE1* would thus restore some of the defects in *mea*.

In the cluster of Type-I AGL proteins identified in our screen we also found a large overlap with genes recently shown to be upregulated in incompatibly balanced *At* x *Aa* crosses compared to semi-compatible *At* x *Aa* maternal excess crosses (*AGL35*, *AGL36*, *PHE1*, *PHE2*, *AGL62*, *AGL90*) [65]. In accordance, mutations of both *AGL62* and *AGL90* partially restore seed lethality in incompatibly balanced *At* x *Aa* crosses, accompanied with selective transmission of the mutant alleles. This array of genes was also found to be upregulated in a PRC2 *fis2* mutant [65]. In addition, *AGL36*, *AGL62*, *AGL90* and *PHE1* were commonly upregulated in transcriptional profiles of *At* paternal excess crosses using tetraploid or unreduced *jason (jas)* pollen [66].

Together with these recent findings, the network of interactions with AGL62 (AGL36, PHE1, PHE2, AGL90) and PHE1 (AGL40, AGL62) and interactors of these proteins (AGL40, AGL45 and AGL90) strongly suggest that the here identified cluster of Type-I AGL proteins plays key roles in parent-of-origin dependent regulation of seed development. An in-depth study of different members of this group will therefore be of great value in understanding this process, and aid the identification of novel imprinted genes.

AGL36 imprinting requires MET1

Here, we report that *AGL36* is a novel imprinted gene that is only expressed from its maternal allele in the endosperm. Silencing of the paternal allele requires the action of MET1, as paternal expression is restored in *met1* mutants.

In public high-density DNA methylation maps prepared from wild-type seedlings (http://signal.salk.edu), both the *AGL36* transcribed region and the 5′ and 3′ regulatory regions are decorated by CG methylation. In line with this, *AGL36* was expressed at very low levels in vegetative tissues. Transcript levels however, were highly elevated in the absence of MET1, in accordance with the virtual absence of CG methylation in *met1* mutants (http://signal.salk.edu) [67].

AGL36 is expressed from both parental alleles at low levels in vegetative tissues, which show that *AGL36* imprinting occurs specifically in the endosperm. Other imprinted genes in *Arabidopsis* have been shown to have biallelic expression in the embryo and other vegetative tissues [11,34,68]. However, for most imprinted genes this issue is not clarified [3]. Since paternal *AGL36* expression is absent in the seed, it suggests that further silencing of *AGL36* takes place by entry into the male germline. Moreover, silencing in the female germline must be lifted to allow *AGL36* expression in the seed. Alternatively, maintenance methylation

and further silencing do not take place on the *AGL36* gene in the female gametophyte. The majority of previously described imprinted genes are regulated by a dual switch of methylation and demethylation involving MET1 and DME [11,18–20,35]. Here we have shown that *AGL36* expression is reduced in a *dme* mutant, indicating that DME has an activating function towards *AGL36*. In accordance with this, mutants of *CMT3*, *KYP*, *AGO4*, *DDM1* and *DRM1/2* had no effect on paternal *AGL36* expression suggesting that maintenance and repression by MET1 and activation by DME is sufficient for *AGL36* imprinting.

In our SNP analyses, a weak paternal signal was observed only at the 2DAP stage. This was interpreted as an artifact since the signal was absent both before and after this stage. If this is a real paternal signal, it suggests an alternative hypothesis where silencing is achieved in the endosperm post fertilization. Further analyses are however required to support this.

In two recent studies, the genome-wide methylation profile of the seed was dissected by comparing cytosine methylation in wild-type embryos to wild-type and *dme* endosperm. This showed that endosperm development, and hence the activity of endosperm-specific genes, is marked by an extensive demethylation of the maternal genome, especially at specific transposon sequences [35,69]. According to the Zilberman Lab Genome Browser (http://dzlab.pmb.berkeley.edu/browser/), such demethylation indeed takes place in the 5′ and 3′ regulatory regions of *AGL36*. Methylation patterns are regained in the *dme* mutant, supporting our data that *AGL36* is maternally activated through the action of DME.

In an elegant approach by Gehring and colleagues, novel imprinted genes have recently been identified by the prediction of *Differentially Methylated Regions* (*DMRs*) between embryo and endosperm. In support of our findings, significant *DMRs* were also mapped to 5′ and 3′ region regions of *AGL36* [35].

Imprinting could be demonstrated in transgenic *pAGL36::GUS* seeds, thus indicating that the 1752 bp promoter fragment used is sufficient for parent-of-origin specific expression. The genomic environment of imprinted genes is highly correlated with transposable elements (TE), and imprinting has been postulated to be an evolutionary byproduct of silencing of invading transposons [23,69,70]. For instance, methylation of a SINE-related tandem repeat structure in the 5′-region correlates with *FWA* expression [32,71], and *DMRs* in *MEA*, *PHE1*, *HDG3* and *HDG9* map to TE [35]. In line with this, a variety of remnants of TE reside in both the 5′ and 3′ regulatory regions of *AGL36* (Figure 4A). The 1752 bp *pAGL36::GUS* promoter fragment harbors remnants of Helitrons and parts of an Arnoldy TE. An 800 bp *DMR* maps immediately (78 bp) upstream of the *AGL36* transcriptional start site overlapping the Helitron TEs ([35], Mary Gehring, personal communication). Clearly, the 1752 bp 5′ region is sufficient for basal *AGL36* imprinting, and similar to the abovementioned examples, *AGL36 DMRs* map to TE. Further investigations will be needed to elucidate the role and the mechanisms of additional 5′ and 3′ *DMRs* as well as the involvement of small RNAs in *AGL36* imprinting [72].

The PRC2 FIS-complex regulates maternal expression of AGL36

Distinct from the expression pattern of *AGL36* that subsides at the time of cellularization in wild-type seeds, *AGL36* maternal expression in *mea* mutant seeds was highly elevated and sustained throughout seed development. Recently, Walia et al. also reported *AGL36* upregulation obtained in five days old seeds from selfed *fis2*^{+/−} plants [65]. Our results show that FIS-complex mediated repression acts exclusively on the expression of the maternal allele

of *AGL36*. The paternal allele was efficiently silenced throughout endosperm development.

Surprisingly, weak paternal *pAGL36::GUS* expression could be observed in 6 DAP early heart stage embryos when the mother was homozygous for *mea*. *MEA* has been shown to have biallelic expression in the embryo [28], and thus the observed paternal expression in hemizygous *mea* embryos is not caused by the lack of functional MEA. This could hint to dosage-dependent regulation of paternal *AGL36* expression by MEA, directly or indirectly, but in lack of further experiments this remains speculation.

Different PRC2 complexes can regulate common genes [30]. However, in mutants of *CLF* and *SWN*, the paralogues of *MEA*, no significant effect on *AGL36* expression levels was found, indicating that *AGL36* regulation is specific to PRC2^FIS. H3K27 trimethylation mediates PRC2s repressive function, and in a whole-genome assay for H3K27 methylation more than 4400 target genes were detected [73] (Daniel Bouyer, personal communication). *AGL36* was however not part of this set of genes. Since this material was obtained from seedlings and may not reflect the situation in the seed, it is not known whether *AGL36* is a direct target of H3K27 trimethylation.

AGL36 identifies a dual regulation mechanism by DME and the FIS PRC2-complex

Repression of the maternal *AGL36* allele identifies a novel means of dual epigenetic regulation of imprinted genes. In this scenario, the expressed maternal *AGL36* allele is antagonistically activated by DME and repressed by PRC2^FIS. To our knowledge, this is the first report of an imprinted gene where the expressed allele is concurrently regulated by a repressive epigenetic mark.

We asked whether this type of regulation was specific for *AGL36* by investigating the *fis* mutant for expression of three other imprinted genes that are activated by DME. We found that these genes fall into two distinct groups; *FWA* and *FIS2* which were largely unaffected by the lack of FIS, and *MPC* along with *AGL36* which showed strong upregulation. This suggests that additional PRC2 regulation of DME-activated alleles defines a common mechanism that applies to a subset of imprinted genes.

In *Arabidopsis*, three imprinted genes, *MEA*, *PHE1* and *AtFH5* are known to have their silenced allele repressed by PRC2^FIS, and two of these genes, *MEA* and *PHE1* are additionally regulated by DNA methylation [55]. In these cases however, the repressed allele is silenced by PRC2 whereas the active allele is regulated by DNA methylation [74]. Here, we show that *AGL36* defines a novel type of regulation where the same allele is activated by DME and repressed by PRC2^FIS in a sequential fashion. This suggests that maternal *AGL36* expression after DME activation needs to be dampened and developmentally regulated by PRC2^FIS, in accordance with the strong *AGL36* expression observed in hypomethylated *met1*^{-/-} plants. Interestingly, DME is required to activate both PRC2^MEA and *AGL36*, and is thus a key player in developmental tuning of parent-of-origin specific *AGL36* expression.

The role of AGL36 in seed development

AGL36 was identified in our transcript profiling as a downregulated gene when the paternal contribution to the endosperm was absent. A simple hypothesis to account for this regulation would be that *AGL36* is under the control of one or more paternally expressed factor(s) that activate the maternal allele of *AGL36*. The identity of such factor(s) remain unknown, and was not approached in this work, but a simple prediction from this hypothesis is that *AGL36* would be upregulated in paternal excess interploidy crosses. In a recent report, *AGL36* is indeed upregulated in such crosses, as well as in crosses with unreduced

diploid *jas* pollen [66]. Such parental cross-talk is however likely to involve complex genetic and epigenetic regulatory mechanisms, and the mechanism that cause the observed transcriptional response of *AGL36* and other previously described imprinted genes in *cdka;1*^b seeds remains to be clarified.

In our study, we have shown that *AGL36* is only maternally expressed. Our current model suggests that the paternal allele is silenced by the action of MET1 and the maternal allele activated by DME (Figure 8). In addition, we have also shown that PRC2^FIS regulates the expression of the maternal *AGL36* allele at the transition between proliferation and cellularization (Figure 8).

Although *AGL36* is identified as a novel target of the imprinting machinery in *Arabidopsis*, we have limited knowledge about its function during plant and seed development. Since expression of *AGL36* and its interacting partners coincide with the transition of endosperm from proliferation to differentiation, we speculate that it plays an important role in this process. This is in agreement with recent findings [65], showing that suppression of an *AGL* cluster including *AGL36* is critical for successful transition of endosperm from syncytial to cellularized stage.

In this work we have identified a novel imprinted gene that is controlled by a novel type of dual epigenetic regulation in the seed. This underscores the importance of further investigations to identify imprinted genes in order to unravel the complex network of epigenetic regulation of parent-of-origin effects in seed development.

Materials and Methods

Plant strains and growth conditions

All plant lines used in these experiments were obtained from the Nottingham Arabidopsis Stock Centre (NASC) unless otherwise stated. The mutant lines *cdka;1-1* (SALK_106809; [40,41]), *ddm1-2* (a kind gift from E. Richards; [53]), *dme-6* (GK-252E03-014577; Figure S9), *mea-8* (SAIL_55_C04; [75]), *mea-9* (SAIL_724_E07; Figure S9), *met1-4*; (SAIL_809_E03; [76] and *swn-4* (SALK_109121; [77]) were in the Col accession. The mutant lines *ago4-1* (N6364; [78]), *clf-2* (N290; [79]), *cmt3-7* (N6365; [80]), *fis1* (a kind gift from A. Chaudhury; [14]) and *kyp-2* (N6367; [51] were in the L*er* accession. The *drm1;drm2* (N6366; [81]) line was in the Ws-2 accession. Mutants used in this study were genotyped using gene-specific and T-DNA specific primers as described in Table S2. The *ddm1-2* mutant line was genotyped by an allele-specific PCR test using dCAPS primers DDM1f and ddm1-2Rsa, as described by [68], allowing digestion of the PCR fragment of the *ddme1-2* allele with RsaI restriction endonuclease, generating a ~130 bp band.

We obtained the *agl36-1* allele from the Koncz collection [48]. Allele-specific PCR, using the primers HOOK1 (left border T-DNA primer) and AGL36-AS2-KONCZ (genomic *AGL36* primer), was carried out to verify the T-DNA insertion, followed by sequencing analysis of the PCR product using the HOOK1 primer. The left border of the insertion was verified to be 16 bp upstream of the ATG start codon of *AGL36*. In addition, there is an 11 bp long DNA filler located between the genomic sequence and the T-DNA sequence.

Arabidopsis seeds were surface-sterilized using EtOH, bleach and Tween20 prior to plating out on MS-2 plates [82] supplemented with 2% Sucrose, containing the correct selection when necessary. Seeds on the MS-2 plates were stratified at 4°C O.N before they were incubated for 14 days at 18°C to germinate. The seedlings were then put on soil and grown in long day conditions (16 hr light) at 18°C.

Seed isolation, RNA extraction, and cDNA synthesis

To increase tissue specificity, siliques were cut open and seeds were isolated directly in tubes containing pre-chilled ceramic
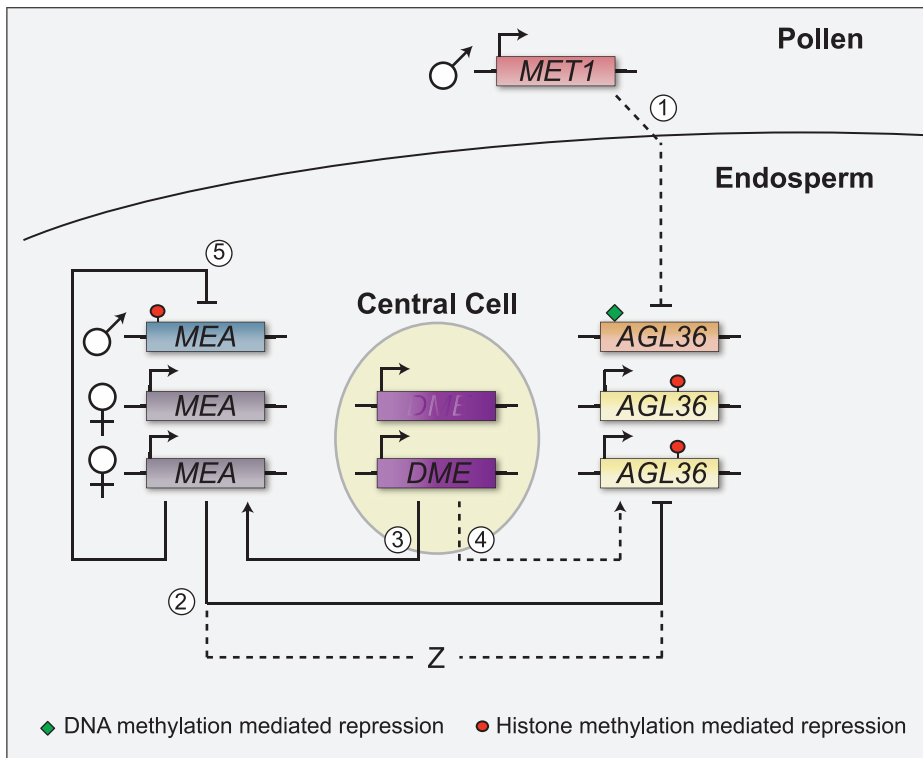
Figure 8. A model for the imprinted expression of *AGL36*. Paternal silencing of *AGL36* is maintained by the action of MET1 in the male germline prior to fertilization (1). The maternal copy of *AGL36* is repressed after fertilization, either directly or indirectly, by the maternally expressed FIS-complex (2) (only MEA is indicated in the figure). *DME* is expressed only in the central cell and activates the maternal allele of *MEA* and *AGL36* (3 & 4). The autoregulatory repression of maternal MEA upon paternal *MEA* is indicated (5). Solid lines indicate direct regulation. Dashed lines indicate possible indirect regulation.
doi:10.1371/journal.pgen.1001303.g008

beads (Roche MagNA Lyser Green Beads). Isolated tissues were stored at $-80°C$. Homogenization was performed by the addition of Lysis buffer containing β-ME (Sigma Spectrum Plant Total RNA Kit) directly to the samples, followed by 3×15 second intervals of homogenization using a MagNA Lyser Instrument (Roche). To prevent RNA degradation, samples were chilled on ice two minutes between each homogenization interval. After the last homogenization step, the samples were centrifuged at $4°C$ for one minute prior to the transfer of the lysate to a new 1.5 ml tube. RNA extraction was performed according to the Sigma Plant Total RNA Kit protocol, except that all centrifugation steps were done at $4°C$ and not at room temperature as indicated in the protocol. RNA was eluted in 50 µl volume. cDNA was synthesized by first preparing the RNA for real-time PCR by treatment with DNase I (Sigma) followed by Reverse Transcription using Oligo(dT) and SuperScript III Reverse Transcriptase (Invitrogen) according to the manufacturer's protocols. The synthesized cDNA was purified utilizing QIAquick PCR Purification kit (Qiagen) and eluted in 30 µl volume prior to measurement of cDNA concentration using a NanoDrop 1000 Spectrophotometer.

Microarray analysis

Plants were grown and seeds isolated as described above. Total RNA was isolated as described above. For microarray analysis, three biological replicas were generated, each consisting of approximately 35 hand-pollinated siliques from ten different plants. The microarray experiment was conducted by the NARC Microarray Service in Trondheim. Microarray slides were printed by the Norwegian Microarray Consortium (Trondheim, Norway).

A custom made *Arabidopsis* chip with 32567 unique 70-mer oligo probes was used in the experiments. Total RNA (15 mg) and Super-Script III reverse transcriptase (Invitrogen) were used in a reverse transcription reaction. A 3DNA Array 350 kit with Cy3- and Cy5-labelled dendrimers (Genisphere Inc.) was used for labeling. Hybridizations were performed in a Slide Booster Hybridization Station (Advalytix), and the slides were washed according to the manufacturers' descriptions (Genisphere and Advalytix). The slides were scanned at 10 mm resolution on a G2505B Agilent DNA microarray scanner (Agilent Technologies). The resulting image files were processed using GenePix 5.1 software (Axon Instruments). Spots identified as not found or manually flagged out as bad were filtered out. Spots with more than 50% saturated pixels were also excluded. The data sets were log-transformed and normalized using the print-tip Loess approach [83]. Within-array replicated measurements for the same gene were merged by taking the average between the replicates. The data were then scaled so that all array data sets had the same median absolute deviation. The differentially expressed genes were identified using the Limma software package [84]. The resulting set of *p*-values were used to compute the *q*-values as described [85].

The microarray data generated in this publication have been deposited in NCBI's Gene Expression Omnibus and are accessible through GEO Series accession number GSE24809 (http://www.ncbi.nlm.nih.gov/geo/query/acc.cgi?acc = GSE24809).

Bioinformatics analyses

We defined the following sub-sets for our microarray data (see Table S3): All expressed = all genes having a present call (17223

genes); Down 0.8 = in Ler x *cdka;1* downregulated genes with $q \leq 0.35$ and arithmetic ratio (ar) ≤ 0.8 (602 genes); Up 1.5 = in Ler x *cdka;1* upregulated genes with $q \leq 0.35$ and ar ≥ 1.5 (323 genes); Up 1.2 = in Ler x *cdka;1* upregulated genes with $q \leq 0.35$ and ar ≥ 1.2 (1030 genes). The *q*-value is the false discovery rate (FDR) of the *p*-value, and was adjusted with Storey's *q*-procedure [85]. The threshold for analysis was set to $q \leq 0.35$ since this value detected paternally expressed genes at an arithmetic ratio (ar) ≤ 0.8. A functional classification was done at http://www.arabidopsis.org/ tools/bulk/go/ using the GO-Slim Molecular Function classification system. For the detailed transcription factor analysis we used the Transcription Factor (TF) classification from the *Arabidopsis* transcription factor database (AtTFDB) hosted on the *Arabidopsis* Gene Regulatory Information Server (AGRIS, http://arabidopsis. med.ohio-state.edu/AtTFDB). The MADS TFs were sub-grouped as in de Folter et al [45]. We compared our microarray data with seed expression data generated by the Goldberg & Harada laboratories, available at http://seedgenenetwork.net/analyze? project = Arabidopsis.

For data comparison a reference set of genes was used that contained all genes covered by the Operon chip used in our study (Arabidopsis thaliana 34K NARC serie 8; GEO Platform GPL11051GPL) and the Affimetrix chip used by Goldberg & Harada (Ath1, GEO Platform GPL198). For the Ath1 chip we used the annotation provided by Goldberg & Harada available at http://seedgenenetwork.net/media/Arab_Final_Annotations_09-07-07_completed.txt. For the operon chip we used the current TAIR 9.0 annotation. From these annotations all AGIs for nuclear genes were extracted and the overlap was calculated. This reference set contained 22130 genes.

We used the reference set overlap of the following Goldberg/ Harada datasets for comparison: GH seed = *call all present and experiment in Arabidopsis ATH1 Array/Arabidopsis/Globular Stage/Seed*; GH seed coat = *call all present and experiment in Arabidopsis ATH1 Array/Arabidopsis/Globular Stage/Chalazal Seed Coat or Arabidopsis ATH1 Array/Arabidopsis/Globular Stage/General Seed Coat*; GH endosperm = *call all present and experiment in Arabidopsis ATH1 Array/Arabidopsis/Globular Stage/Chalazal Endosperm or Arabidopsis ATH1 Array/Arabidopsis/Globular Stage/Micropylar Endosperm or Arabidopsis ATH1 Array/Arabidopsis/Globular Stage/Peripheral Endosperm*; GH embryo = *call all present and experiment in Arabidopsis ATH1 Array/Arabidopsis/Globular Stage/Embryo Proper*.

Venn diagrams were generated using the VENN diagram generator designed by Tim Hulsen at http://www.cmbi.ru.nl/ cdd/biovenn/ [86]. The test for statistical significance of the overlap between two groups of genes was calculated by using software provided by Jim Lund accessible at http://elegans.uky. edu/MA/progs/overlap_stats.html.

Plasmid construction

To generate the *pAGL36::GUS* construct we utilized the Gateway cloning technology (Gateway; Invitrogen). The promoter region ($\div$1740–12) spanning the ATG start codon was amplified using the attB sequence containing primers attB1-pAGL36-AS7 and attB2-pAGL36-S4 (Table S2), and cloned into the pMDC162 GUS-vector [87]. The resulting construct, after checking the DNA sequence, was introduced to Col ecotype by *Agrobacterium tumefaciens* mediated transformation using the floral-dip method [88].

β-Glucuronidase expression analysis and histology

Histochemical assays were performed after a modified protocol from Grini *et al.* (2002) by incubating the tissues in staining buffer (2 mM X-Gluc; 50 mM NaPO$_4$, pH 7.2; 2 mM K$_4$Fe(CN)$_6$ x 3H$_2$O; 2 mM K$_3$Fe(CN)$_6$; 0.1% Triton) overnight at 37°C before the reaction was terminated using 50% EtOH. The tissues were cleared and mounted on slides according to Grini *et al.* (2002), and inspected using an Axioplan 2 Carl Zeiss Microscope. Images were acquired with an AxioCam HRc Carl Zeiss camera and processed with AxioVs40 V 4.5.0.0 software.

Real-time quantitative PCR

Real-time PCR was performed using a Light-cycler LC480 instrument (Roche) according to the manufacturer's protocol. To ensure high PCR efficiency and to avoid undesired primer dimers, all oligonucleotide pairs were initially tested by melting point analysis using SYBR Premix Ex Taq (TaKaRa). To obtain higher level of gene specificity, probe-based real-time PCR with confirmed primers were performed using Universal Probe Library (UPL) hydrolysis probes (Roche) in combination with Premix Ex Taq (TaKaRa).

For *AGL36* real-time PCR, we used primers AGL36-160-LP and AGL36-160-RP, which gave a 60 bp amplicon (Table S2). Comparison of the sequences of the coding region and the 3′UTR of *AGL36* with *AGL34* and *AGL90*, revealed more than 85% and 84% sequence similarity respectively between these genes (Figure S8). To ensure that the abovementioned primers are only amplifying *AGL36*, we cloned the obtained amplicon from four independent reactions into the pCR2.1 vector (Invitrogen), and subsequently sequenced two clones of each construct with M13-Forward and M13-Reverse primers. Sequence results revealed exclusive and specific *AGL36* amplification.

ACTIN11 (*ACT11*), a housekeeping gene that is strongly expressed in the developing ovules [89], was shown in a preliminary analysis not to be affected by our experimental conditions (data not shown), and was therefore selected as a reference gene. *GLYCERALDEHYDE-3-P DEHYDROGENASE A-SUBUNIT* (*GAPA*) was used as an additional reference gene. The oligo sequences, their amplicons and appropriate UPL probes are shown in Table S2.

Real-time PCR of all samples and reference controls were performed in two independent biological replicates and repeated at least two times (technical replicas) unless otherwise stated. The PCR efficiency was determined independently for all replicates (biological and technical) by series of dilutions (100 ng, 50 ng, 20 ng, 5 ng template/rxn) for each experiment. This allowed us to obtain the efficiency for each single reaction. Calculations of relative expression ratios were performed according to a model described by Pfaffl [90] with minor exceptions. Since we had efficiency for all reactions (four values for each calculation corresponding to $E^{\text{target-sample}}$, $E^{\text{target-standard}}$, $E^{\text{reference-sample}}$ and $E^{\text{reference-standard}}$), we calculated the average E^{target} and $E^{\text{reference}}$ values from the standards and the samples, ending up with two E-values that we could use in the formula described by Pfaffl.

Single Nucleotide Polymorphism analysis

RNA was isolated and cDNA synthesized and purified as described above. Polymorphisms between various ecotypes were identified using TAIR Genome Browser (www.arabidopsis.org) and/or the *Arabidopsis* SNP Sequence Viewer tool provided by the Salk Institute Genomic Analysis Laboratory (http://natural.salk. edu/cgi-bin/snp.cgi). A selected region spanning the SNP of interest was amplified by PCR using TaKaRa Ex Taq DNA polymerase applying 100 ng template per reaction, and the following PCR parameters in a 50 µl reaction: 94°C-3 min, 35×(94°C-1 min, 58°C-30 sec, 72°C-1 min/kb), 72°C-5 min, 4°C-∞. Parental-specific expression based on SNP was determined by setting up an appropriate restriction digest. For *AGL36* SNP analysis, 20 µl of the SNP PCR reaction was digested with 15 U of

*Alw*NI at 37°C for a duration of 2.5 hrs, followed by a 20 min inactivation at 65°C. For the *FWA* control SNP, due to the absence of a restriction site in the SNP region in both Col and L*er* ecotypes, dCAPS primers were used, generating a *Nhe*I restriction site in the Col ecotype. The obtained amplicons for both ecotypes were digested with *Nhe*I [11].

In cases where the detected SNP did not result in digestion in neither ecotype, a primer sequence was designed to introduce a base exchange adjacent to the SNP, leading to restriction digestion of one of the ecotypes. The obtained amplicon for both ecotypes were then treated with the appropriate restriction enzyme. In all experiments either genomic DNA or cDNA from wild-type plants from both ecotypes used in the study was used as controls for the presence or absence of digestion. The digested samples were analyzed using DNA-1000-LabOnChip and 2100 Bioanalyzer (Agilent Technologies).

To rule out that the primers used for *AGL36* SNP PCR (AGL36-SP7-SNP and AGL36-ASP6-SNP) (Table S2) would amplify the highly similar *AGL90*, we oriented the AGL36-SP7-SNP primer such that it was located in a region that was annotated as intron in *AGL90* but not in *AGL36* (Figure S8). First, the presence of the intron in *AGL90* was confirmed by amplifying the intron-flanking region (AGL90-SP1-subcloning and AGL90-ASP2-subcloning primers (Table S2)), and comparing the size differences obtained between the genomic PCR and cDNA PCR. Due to high sequence similarity, we suspected to amplify both *AGL36* and *AGL90* in these PCR reactions. To distinguish between these two amplicons, we took advantage of the presence of two unique restriction sites (*Msl*I and *Bsp*BI) in the amplified region of *AGL36* that are absent in *AGL90*.

Sequence comparison between the abovementioned *AGL36*-SNP primers and *AGL34* showed that there was approximately 70% and 91% sequence similarity between the primers and the *AGL34* gene. However, if these primers were functional in amplifying *AGL34*, they would result in a smaller amplicon than *AGL36* amplicon (373 bp versus 399 bp respectively). This difference could easily be detected using a DNA-1000-LabOnChip. Our SNP data only showed the expected 399 bp band, verifying that *AGL34* was not amplified using the above primers. The paternally imprinted *FWA* gene was used as a positive control by utilizing primers FWA-RTf and FWA-dNheI (Table S2) for PCR amplification followed by *Nhe*I restriction digest.

Supporting Information

Figure S1 Genomic dissection of parental effects using *cdka;1* as a tool. (A–D) Basic setup and hypothetical outcome of the L*er* x Col vs. L*er* x *cdka;1* microarray screen. (A) Transcription profiles from L*er* x Col seeds were compared to L*er* x *cdka;1*. In the endosperm of L*er* x *cdka;1* no paternal genome is present. (B) Paternally expressed target genes will be absent in L*er* x *cdka;1* seeds and thus downregulated. (C) Target genes that are activated by a paternally expressed gene *X* will be silent without the activator present, and thus downregulated. (D) If repressed by a paternally expressed gene *X*, the target gene will be upregulated. (E) Previously identified imprinted genes display reduced expression in *cdka;1* fertilized seeds with no paternal contribution to the endosperm. Paternally expressed genes are shown in the upper panel. Maternally expressed genes are shown in the lower panel. The *q*-value (1) is defined to be the false discovery rate (FDR) of the *p*-value, and was adjusted with Storey's *q*-procedure [85]. The seed expression profile (2), obtained from Genevestigator, is showing the level of gene expression in the embryo, the endosperm (micropylar, peripheral, and chalazal), the seed coat and the

suspensor. The expression levels are shown in a range from low/none (white) to high (dark blue). The probe for the *PHE1* and *PHE2* expression profile is not able to distinguish between these genes and is represented with **.
Found at: doi:10.1371/journal.pgen.1001303.s001 (1.72 MB EPS)

Figure S2 Overlap between different seed compartment profiles and *cdka;1* microarray expression data. (A) Venn diagrams representing overlap of genes expressed at globular stage in endosperm, seed coat or embryo of *Arabidopsis* Ws-0 plants (grey/white) and genes expressed in 3 DAP seeds from L*er* plants pollinated with Col *cdka;1* pollen (green). Genes significantly deregulated with respect to seeds from L*er* plants pollinated with Col pollen are indicated in blue (downregulation, ar ≤0.8), red (upregulation, ar ≥1.5) and orange (upregulation ar ≥1.2). Gene numbers refer to the reference set of genes (see material and methods). GH endosperm represents expression in chalazal or micropylar or peripheral endosperm, GH seed coat represents expression in chalazal or general seed coat (www.seedgenenet work.net). GH: Goldberg & Harada laboratories. (B) Two groups of genes are compared and found to have x genes in common. A representation factor (rf) and the probability (p) of finding an overlap of x genes are calculated at http://elegans.uky.edu/MA/progs/overlap_stats.html. The representation factor is the number of overlapping genes divided by the expected number of overlapping genes drawn from two independent groups. A representation factor >1 indicates more overlap than expected of two independent groups, a representation factor <1 indicates less overlap than expected. The overlap of the L*er* x *cdka;1* seed dataset (green) with each of the GH datasets (grey/white) is always rf = 1.3 with a p-value of <1.0 e -99 (highly significant, below calculation limit of the software). For all other comparisons see table. ar: arithmetic ratio of expression values (L*er* x *cdka;1*/L*er* x Col).
Found at: doi:10.1371/journal.pgen.1001303.s002 (0.39 MB EPS)

Figure S3 Differences in deregulation in L*er* x *cdka;1* seeds among the different transcription factor families. On the X-axis the different transcription factor (TF) families are listed, the Y-axis displays the amount of TFs as absolute numbers (A) or as percentage with respect to all seed-expressed TFs in each class (B). Green bars represent all TFs having a present call in our microarray experiment, blue bars indicate TFs that are downregulated (cut-off ≤0.8) and red and orange bars indicate the TFs that are upregulated in L*er* x *cdka;1* seeds at 3 DAP (cut-off ≥1.5 or 1.2 respectively). The MADS Mγ TFs are the most strongly downregulated class in absolute numbers as well as in percentage.
Found at: doi:10.1371/journal.pgen.1001303.s003 (0.44 MB EPS)

Figure S4 Downregulated AGAMOUS-LIKE (AGL) transcription factors. Upper panel: MADS-box transcription factors identified in genome-wide transcript profiling of endosperm without paternal contribution. The table shows all identified MADS-box genes with a cut-off at >0.8-fold downregulation. The logarithmic and arithmetic relative expression ratios are indicated. The Mα and the Mγ Type-I subclass of MADS-box factors are indicated in blue and green respectively. The Type-II MADS-box factor is indicated in yellow. The *p*-value (1) (a score between 0 and 1) is the likelihood of an event. The *q*-value (2) is defined to be the false discovery rate (FDR) of the *p*-value, and was adjusted with Storey's *q*-procedure [85]. The seed expression profile (3), obtained from Genevestigator, is showing the level of gene expression in the embryo, the endosperm (micropylar, peripheral, and chalazal), the seed coat and the suspensor. The expression levels are shown in a range from low/none (white) to high (dark blue). The probe for the expression profile of *AGL36* and *AGL90* is

not able to distinguish between these genes and is represented with *. The probe for *PHE1* and *PHE2* expression profile is also not able to distinguish between these genes and is represented with **. Lower panel: Map of interactions between selected AGL proteins, modified from de Folter, 2005 [46], and the Bio-Array Resource (BAR) Arabidopsis Interaction Viewer (http://bar.utoronto.ca/). Blue ring color indicates the Mα subclass while green ring color indicates Mγ subclass. Genes identified in our microarray (pink fill) and their interacting partners (no fill) are visualized.

Found at: doi:10.1371/journal.pgen.1001303.s004 (0.41 MB EPS)

Figure S5 Analysis of the *agl36-1* T-DNA insertion line. (A) T-DNA insertion map of *agl36-1*. The KONCZ T-DNA is inserted 16 bp upstream of ATG. There is an 11 bp DNA filler positioned between the T-DNA insert and the genomic *AGL36* sequence (asterisk). The position of the left border (LB) of the insertion was verified by PCR using primers HOOK1 and AGL36-AS2-KONCZ. (B) Real-time PCR of *AGL36* expression levels in 3 DAP seeds of *agl36-1* hemizygous and homozygous plants, relative to wild-type Col seeds. The graph represents the average relative expression values from two independent biological parallels where each gave rise to two independent technical replicas. STDEVs are derived from the independent biological parallels. The *AGL36* transcript levels were normalized to *ACT11* levels. (C) Phenotypic analysis of wild-type Col (upper panel) and *agl36-1*$^{-/-}$ (lower panel) seeds. Samples are taken at 2, 4 and 6 DAP. There is no obvious mutant phenotype observed in the seed and the developing embryo. (D) Histochemical detection of GUS activity in *agl36-1*$^{+/-}$ seeds expressing a maternal *pFIS2::GUS* construct. The division pattern and the nuclear migration is similar to that of wild-type seeds (not shown).

Found at: doi:10.1371/journal.pgen.1001303.s005 (1.65 MB TIF)

Figure S6 The effect of maternal DNA methylation on *AGL36* expression. SNP analyses of 3 DAP seeds from crosses with DNA methylation mutants. The cross is reciprocal of the results presented in Figure 5A. The amplified SNP containing a region of *AGL36* cDNA was digested with *Alw*NI and analyzed in a Bioanalyzer. Homozygous *cmt3-7*, *kyp-2*, and *ago4-1* mutants in the L*er* ecotype were pollinated with Col plants, while homozygous *drm1;drm2* mutants in the Ws-2 ecotype were pollinated with L*er* plants. No paternal *AGL36* expression could be detected in these crosses.

Found at: doi:10.1371/journal.pgen.1001303.s006 (0.49 MB EPS)

Figure S7 *pAGL36::GUS* in reciprocal crosses and *mea* background. (A) *pAGL36::GUS* used as the paternal pollen donor on *mea*$^{-/-}$. Note: Weak expression in the 6 DAP embryo. (B) *mea*$^{+/-}$; *pAGL36::GUS* plants crossed with wild-type pollen. An increased *pAGL36::GUS* expression is detected in the *mea* background. (C) Wild-type plants are crossed with *mea*$^{+/-}$;*pAGL36::GUS* pollen. No expression is detected. (D) Wild-type pollen from Col ecotype was used to fertilize plants expressing *pAGL36::GUS*. Maternal expression is detected. (E) Plants expressing *pAGL36::GUS* were used as paternal partners in crosses with wild-type Col plants. No paternal expression is detected. Samples are taken at 3 DAP (left panel) and 6 DAP (right panel).

Found at: doi:10.1371/journal.pgen.1001303.s007 (6.64 MB TIF)

Figure S8 *AGL36* alignment with *AGL34* and *AGL90*. Alignment of the transcribed and 3′UTR regions of *AGL34*, *AGL36* and *AGL90*. The ATG start and TAA stop codons are marked with red boxes. Sequence similarity between all three genes is shown in black (and shown with capital letters below the alignment), whereas similarity between two genes is indicated with gray (and shown in small letters below the alignment). Gaps are shown with dashed lines. The forward and reverse oligonucleotide sequences for *AGL36* real-time PCR (AGL36-160-LP and AGL36-160-RP) are shown in red letters and indicated with (A) and red lines above the sequence. The corresponding UPL Probe #160 sequence is shown with orange letters and indicated with (B) and an orange line above the sequence. *AGL90* intron is indicated with (C) and shown with black text and blue background color. The forward and reverse oligonucleotide sequences for *AGL36* SNP analysis (AGL36-SP7-SNP and AGL36-ASP6-SNP) are shown in green letters and indicated with letter (D), and green lines above the sequence. Note: The reverse AGL36-ASP6-SNP primer is located in the 3′UTR. The forward and reverse primers for *AGL90* amplification flanking the introns are indicated with black text and yellow background (E).

Found at: doi:10.1371/journal.pgen.1001303.s008 (8.61 MB TIF)

Figure S9 Description of *mea-8*, *mea-9* and *dme-6* T-DNA insertion lines. (A) T-DNA insertion map of *mea-8* (SAIL_55_C04, [75]) and *mea-9* (SAIL_724_E07) mutant lines. The T-DNA is inserted in the 4th and the 6th intron respectively. A phenotypic characterization was performed on *mea-9* mutant seeds (right) and compared to wild-type seeds (left) at 12 DAP. The *mea-9* line displays the same arrested phenotype as previously described, and arrests at late heart stage of embryo development. The frequency of aborted seeds (see table) is similar to previously described *mea* alleles. (B) T-DNA insertion map of *dme-6* (GK-252E03-014577) mutant line. The GABI-KAT T-DNA is inserted in the 2nd intron. A phenotypic characterization was performed on *dme-6* mutant seeds (lower panel) and compared to wild-type seeds (upper) at 9 and 12 DAP. The *dme-6* mutant displays a characteristic maternal gametophytic abortion phenotype with enlarged endosperm and an aborting embryo at late heart stage. The abortion rate of the mutant ovules is approximately 50%. (C) Real-time PCR expression analysis in mutant lines. The expression level of *PHE1*, which is repressed by *MEA*, is increased in both *mea-8* and *mea-9* mutant lines. The expression level of *PHE1* in *dme-6* increase at 6 DAP since *DME* activate *MEA* expression.

Found at: doi:10.1371/journal.pgen.1001303.s009 (7.57 MB EPS)

Table S1 Segregation and reciprocal crosses of the *agl36-1* mutant line. ^{1}Number of hygromycin resistant and sensitive plants in self-fertilized and reciprocally crossed plants. ^{2}Percent hygromycin resistant plants in self-fertilized and reciprocally crossed plants. Standard deviation is indicated in this field. ^{3}Mean percent value for resistant plants in self-fertilized and reciprocally crossed plants. ^{4}Median percent value for resistant plants in self-fertilized and reciprocally crossed plants. ^{5}Chi-square test: H$_0$: 75% segregation in hemizygous self-fertilized plants or 50% segregation in hemizygous outcrossed plants. A P value of 0,05 with 1 degree of freedom was used, meaning that with $\chi^2 < 3,84$, the hypothesis holds with 95% accuracy, and is not rejected.

Found at: doi:10.1371/journal.pgen.1001303.s010 (0.44 MB EPS)

Table S2 Primer sequences and Real-time PCR probes. Oligo sequences are all given in 5′–3′ direction. See comments in the table for details.

Found at: doi:10.1371/journal.pgen.1001303.s011 (0.08 MB PDF)

Table S3 Gene lists—evaluation of microarray expression data. The following gene sets extracted from our microarray experiments are shown: *All expressed* = all genes having a present call (17223 genes); *Down 0.8* = in L*er* x *cdka;1* downregulated genes with q ≤ 0.35 and arithmetic ratio (ar) ≤ 0.8 (602 genes); *Up 1.5* = in L*er* x *cdka;1* upregulated genes with q ≤ 0.35 and ar ≥ 1.5 (323 genes); *Up 1.2* = in L*er* x *cdka;1* upregulated genes with q ≤ 0.35

and ar ≥ 1.2 (1030 genes). The raw data for the microarray experiments can be downloaded from GEO (GEO Series GSE24809).

Found at: doi:10.1371/journal.pgen.1001303.s012 (3.18 MB XLS)

Acknowledgments

Author Contributions

Conceived and designed the experiments: PEG. Performed the experiments: RS EDA KNB BMG AU. Analyzed the data: RS EDA KNB BMG MH AU PW AS PEG. Contributed reagents/materials/analysis tools: CK RBA AS. Wrote the paper: RS AS PEG.

References

1. Nowack MK, Ungru A, Bjerkan KN, Grini PE, Schnittger A (2010) Reproductive cross-talk: seed development in flowering plants. Biochem Soc Trans 38: 604–612.
2. Feil R, Berger F (2007) Convergent evolution of genomic imprinting in plants and mammals. Trends Genet 23: 192–199.
3. Jullien PE, Berger F (2009) Gamete-specific epigenetic mechanisms shape genomic imprinting. Curr Opin Plant Biol 12: 637–642.
4. Lin BY (1984) Ploidy Barrier to Endosperm Development in Maize. Genetics 107: 103–115.
5. Scott RJ, Spielman M, Bailey J, Dickinson HG (1998) Parent-of-origin effects on seed development in *Arabidopsis thaliana*. Development 125: 3329–3341.
6. Haig D, Westoby M (1991) Genomic Imprinting in Endosperm: Its Effect on Seed Development in Crosses between Species, and between Different Ploidies of the Same Species, and Its Implications for the Evolution of Apomixis. Philosophical Transactions: Biological Sciences 333: 1–13.
7. DeChiara TM, Efstratiadis A, Robertson EJ (1990) A growth-deficiency phenotype in heterozygous mice carrying an insulin-like growth factor II gene disrupted by targeting. Nature 345: 78–80.
8. Filson AJ, Louvi A, Efstratiadis A, Robertson EJ (1993) Rescue of the T-associated maternal effect in mice carrying null mutations in Igf-2 and Igf2r, two reciprocally imprinted genes. Development 118: 731–736.
9. Lau MM, Stewart CE, Liu Z, Bhatt H, Rotwein P, et al. (1994) Loss of the imprinted IGF2/cation-independent mannose 6-phosphate receptor results in fetal overgrowth and perinatal lethality. Genes Dev 8: 2953–2963.
10. Leighton PA, Ingram RS, Eggenschwiler J, Efstratiadis A, Tilghman SM (1995) Disruption of imprinting caused by deletion of the H19 gene region in mice. Nature 375: 34–39.
11. Kinoshita T, Miura A, Choi Y, Kinoshita Y, Cao X, et al. (2004) One-way control of *FWA* imprinting in *Arabidopsis* endosperm by DNA methylation. Science 303: 521–523.
12. Lawrence RJ, Earley K, Pontes O, Silva M, Chen ZJ, et al. (2004) A concerted DNA methylation/histone methylation switch regulates rRNA gene dosage control and nucleolar dominance. Mol Cell 13: 599–609.
13. Grossniklaus U, Vielle-Calzada JP, Hoeppner MA, Gagliano WB (1998) Maternal control of embryogenesis by MEDEA, a polycomb group gene in *Arabidopsis*. Science 280: 446–450.
14. Chaudhury AM, Ming L, Miller C, Craig S, Dennis ES, et al. (1997) Fertilization-independent seed development in *Arabidopsis thaliana*. Proc Natl Acad Sci U S A 94: 4223–4228.
15. Ohad N, Margossian L, Hsu YC, Williams C, Repetti P, et al. (1996) A mutation that allows endosperm development without fertilization. Proc Natl Acad Sci U S A 93: 5319–5324.
16. Kohler C, Hennig L, Bouveret R, Gheyselinck J, Grossniklaus U, et al. (2003) *Arabidopsis* MSI1 is a component of the MEA/FIE Polycomb group complex and required for seed development. Embo J 22: 4804–4814.
17. Guitton AE, Page DR, Chambrier P, Lionnet C, Faure JE, et al. (2004) Identification of new members of Fertilisation Independent Seed Polycomb Group pathway involved in the control of seed development in *Arabidopsis thaliana*. Development 131: 2971–2981.
18. Tiwari S, Schulz R, Ikeda Y, Dytham L, Bravo J, et al. (2008) *MATERNALLY EXPRESSED PAB C-TERMINAL*, a novel imprinted gene in *Arabidopsis*, encodes the conserved C-terminal domain of polyadenylate binding proteins. Plant Cell 20: 2387–2398.
19. Jullien PE, Kinoshita T, Ohad N, Berger F (2006) Maintenance of DNA methylation during the *Arabidopsis* life cycle is essential for parental imprinting. Plant Cell 18: 1360–1372.
20. Adams S, Vinkenoog R, Spielman M, Dickinson HG, Scott RJ (2000) Parent-of-origin effects on seed development in *Arabidopsis thaliana* require DNA methylation. Development 127: 2493–2502.
21. Johnston AJ, Matveeva E, Kirioukhova O, Grossniklaus U, Gruissem W (2008) A Dynamic Reciprocal RBR-PRC2 Regulatory Circuit Controls *Arabidopsis* Gametophyte Development. Curr Biol 18: 1680–1686.
22. Jullien P, Mosquna A, Ingouff M, Sakata T, Ohad N, et al. (2008) Retinoblastoma and its binding partner MSI1 control imprinting in *Arabidopsis*. PLoS Biol 6: e194. doi:10.1371/journal.pbio.0060194.
23. Gehring M, Reik W, Henikoff S (2009) DNA demethylation by DNA repair. Trends Genet 25: 82–90.
24. Choi Y, Gehring M, Johnson L, Hannon M, Harada JJ, et al. (2002) DEMETER, a DNA glycosylase domain protein, is required for endosperm gene imprinting and seed viability in *Arabidopsis*. Cell 110: 33–42.
25. Baroux C, Gagliardini V, Page DR, Grossniklaus U (2006) Dynamic regulatory interactions of Polycomb group genes: MEDEA autoregulation is required for imprinted gene expression in *Arabidopsis*. Genes Dev 20: 1081–1086.
26. Fitz Gerald JN, Hui PS, Berger F (2009) Polycomb group-dependent imprinting of the actin regulator *AtFH5* regulates morphogenesis in *Arabidopsis thaliana*. Development 136: 3399–3404.
27. Jullien PE, Katz A, Oliva M, Ohad N, Berger F (2006) Polycomb group complexes self-regulate imprinting of the Polycomb group gene *MEDEA* in *Arabidopsis*. Curr Biol 16: 486–492.
28. Kinoshita T, Yadegari R, Harada JJ, Goldberg RB, Fischer RL (1999) Imprinting of the *MEDEA* polycomb gene in the *Arabidopsis* endosperm. Plant Cell 11: 1945–1952.
29. Kohler C, Hennig L, Spillane C, Pien S, Gruissem W, et al. (2003) The Polycomb-group protein MEDEA regulates seed development by controlling expression of the MADS-box gene *PHERES1*. Genes Dev 17: 1540–1553.
30. Makarevich G, Leroy O, Akinci U, Schubert D, Clarenz O, et al. (2006) Different Polycomb group complexes regulate common target genes in *Arabidopsis*. EMBO Rep 7: 947–952.
31. Scott RJ, Spielman M (2006) Genomic imprinting in plants and mammals: how life history constrains convergence. Cytogenet Genome Res 113: 53–67.
32. Kinoshita Y, Saze H, Kinoshita T, Miura A, Soppe WJ, et al. (2007) Control of *FWA* gene silencing in *Arabidopsis thaliana* by SINE-related direct repeats. Plant J 49: 38–45.
33. Luo M, Bilodeau P, Dennis ES, Peacock WJ, Chaudhury A (2000) Expression and parent-of-origin effects for *FIS2*, *MEA*, and *FIE* in the endosperm and embryo of developing *Arabidopsis* seeds. Proc Natl Acad Sci U S A 97: 10637–10642.
34. Tiwari S, Spielman M, Day RC, Scott RJ (2006) Proliferative phase endosperm promoters from *Arabidopsis thaliana*. Plant Biotechnol J 4: 393–407.
35. Gehring M, Bubb KL, Henikoff S (2009) Extensive demethylation of repetitive elements during seed development underlies gene imprinting. Science 324: 1447–1451.
36. Isles AR, Holland AJ (2005) Imprinted genes and mother-offspring interactions. Early Hum Dev 81: 73–77.
37. Morison IM, Ramsay JP, Spencer HG (2005) A census of mammalian imprinting. Trends Genet 21: 457–465.
38. Reik W, Lewis A (2005) Co-evolution of X-chromosome inactivation and imprinting in mammals. Nat Rev Genet 6: 403–410.
39. Wood AJ, Oakey RJ (2006) Genomic imprinting in mammals: emerging themes and established theories. PLoS Genet 2: e147. doi:10.1371/journal.pgen.0020147.
40. Nowack MK, Grini PE, Jakoby MJ, Lafos M, Koncz C, et al. (2006) A positive signal from the fertilization of the egg cell sets off endosperm proliferation in angiosperm embryogenesis. Nat Genet 38: 63–67.
41. Iwakawa H, Shinmyo A, Sekine M (2006) *Arabidopsis* CDKA;1, a cdc2 homologue, controls proliferation of generative cells in male gametogenesis. Plant J 45: 819–831.
42. Aw SJ, Hamamura Y, Chen Z, Schnittger A, Berger F (2010) Sperm entry is sufficient to trigger division of the central cell but the paternal genome is required for endosperm development in *Arabidopsis*. Development 137: 2683–2690.
43. Nowack MK, Shirzadi R, Dissmeyer N, Dolf A, Endl E, et al. (2007) Bypassing genomic imprinting allows seed development. Nature 447: 312–315.
44. Le BH, Cheng C, Bui AQ, Wagmaister JA, Henry KF, et al. (2010) Global analysis of gene activity during *Arabidopsis* seed development and identification of seed-specific transcription factors. Proc Natl Acad Sci U S A 107: 8063–8070.
45. de Folter S, Immink RG, Kieffer M, Parenicova L, Henz SR, et al. (2005) Comprehensive interaction map of the *Arabidopsis* MADS Box transcription factors. Plant Cell 17: 1424–1433.
46. Kang IH, Steffen JG, Portereiko MF, Lloyd A, Drews GN (2008) The AGL62 MADS domain protein regulates cellularization during endosperm development in *Arabidopsis*. Plant Cell 20: 635–647.
47. Parenicova L, de Folter S, Kieffer M, Horner DS, Favalli C, et al. (2003) Molecular and phylogenetic analyses of the complete MADS-box transcription

factor family in *Arabidopsis*: new openings to the MADS world. Plant Cell 15: 1538–1551.

48. Rios G, Lossow A, Hertel B, Breuer F, Schaefer S, et al. (2002) Rapid identification of *Arabidopsis* insertion mutants by non-radioactive detection of T-DNA tagged genes. Plant J 32: 243–253.

49. Grini PE, Schnittger A, Schwarz H, Zimmermann I, Schwab B, et al. (1999) Isolation of ethyl methanesulfonate-induced gametophytic mutants in *Arabidopsis thaliana* by a segregation distortion assay using the multimarker chromosome 1. Genetics 151: 849–863.

50. Cao X, Jacobsen SE (2002) Locus-specific control of asymmetric and CpNpG methylation by the *DRM* and *CMT3* methyltransferase genes. Proc Natl Acad Sci U S A 99(Suppl 4): 16491–16498.

51. Jackson JP, Lindroth AM, Cao X, Jacobsen SE (2002) Control of CpNpG DNA methylation by the KRYPTONITE histone H3 methyltransferase. Nature 416: 556–560.

52. Chan SW, Zilberman D, Xie Z, Johansen LK, Carrington JC, et al. (2004) RNA silencing genes control de novo DNA methylation. Science 303: 1336.

53. Jeddeloh JA, Stokes TL, Richards EJ (1999) Maintenance of genomic methylation requires a SWI2/SNF2-like protein. Nat Genet 22: 94–97.

54. Day RC, Herridge RP, Ambrose BA, Macknight RC (2008) Transcriptome analysis of proliferating *Arabidopsis* endosperm reveals biological implications for the control of syncytial division, cytokinin signaling, and gene expression regulation. Plant Physiol 148: 1964–1984.

55. Jullien PE, Berger F (2010) Parental genome dosage imbalance deregulates imprinting in *Arabidopsis*. PLoS Genet 6: e1000885. doi:10.1371/journal.pgen.1000885.

56. Kohler C, Page DR, Gagliardini V, Grossniklaus U (2005) The *Arabidopsis thaliana* MEDEA Polycomb group protein controls expression of PHERES1 by parental imprinting. Nat Genet 37: 28–30.

57. Becker A, Theissen G (2003) The major clades of MADS-box genes and their role in the development and evolution of flowering plants. Mol Phylogenet Evol 29: 464–489.

58. Kofuji R, Sumikawa N, Yamasaki M, Kondo K, Ueda K, et al. (2003) Evolution and divergence of the MADS-box gene family based on genome-wide expression analyses. Mol Biol Evol 20: 1963–1977.

59. Bemer M, Wolters-Arts M, Grossniklaus U, Angenent GC (2008) The MADS domain protein DIANA acts together with AGAMOUS-LIKE80 to specify the central cell in *Arabidopsis* ovules. Plant Cell 20: 2088–2101.

60. Portereiko MF, Lloyd A, Steffen JG, Punwani JA, Otsuga D, et al. (2006) AGL80 is required for central cell and endosperm development in *Arabidopsis*. Plant Cell 18: 1862–1872.

61. Colombo M, Masiero S, Vanzulli S, Lardelli P, Kater MM, et al. (2008) *AGL23*, a type I MADS-box gene that controls female gametophyte and embryo development in *Arabidopsis*. Plant J 54: 1037–1048.

62. Steffen JG, Kang IH, Portereiko MF, Lloyd A, Drews GN (2008) AGL61 interacts with AGL80 and is required for central cell development in *Arabidopsis*. Plant Physiol 148: 259–268.

63. De Bodt S, Raes J, Florquin K, Rombauts S, Rouze P, et al. (2003) Genomewide structural annotation and evolutionary analysis of the type I MADS-box genes in plants. J Mol Evol 56: 573–586.

64. Josefsson C, Dilkes B, Comai L (2006) Parent-dependent loss of gene silencing during interspecies hybridization. Curr Biol 16: 1322–1328.

65. Walia H, Josefsson C, Dilkes B, Kirkbride R, Harada J, et al. (2009) Dosage-dependent deregulation of an AGAMOUS-LIKE gene cluster contributes to interspecific incompatibility. Curr Biol 19: 1128–1132.

66. Erilova A, Brownfield L, Exner V, Rosa M, Twell D, et al. (2009) Imprinting of the polycomb group gene *MEDEA* serves as a ploidy sensor in *Arabidopsis*. PLoS Genet 5: e1000663. doi:10.1371/journal.pgen.1000663.

67. Zhang X, Yazaki J, Sundaresan A, Cokus S, Chan SW, et al. (2006) Genome-wide High-Resolution Mapping and Functional Analysis of DNA Methylation in *Arabidopsis*. Cell 126: 1189–1201.

68. Yadegari R, Kinoshita T, Lotan O, Cohen G, Katz A, et al. (2000) Mutations in the *FIE* and *MEA* genes that encode interacting polycomb proteins cause parent-of-origin effects on seed development by distinct mechanisms. Plant Cell 12: 2367–2382.

69. Hsieh TF, Ibarra CA, Silva P, Zemach A, Eshed-Williams L, et al. (2009) Genome-wide demethylation of *Arabidopsis* endosperm. Science. pp 1451–1454.

70. Barlow DP (1993) Methylation and imprinting: from host defense to gene regulation? Science 260: 309–310.

71. Chan SW, Zhang X, Bernatavichute YV, Jacobsen SE (2006) Two-step recruitment of RNA-directed DNA methylation to tandem repeats. PLoS Biol 4: e363. doi:10.1371/journal.pbio.0040363.

72. Mosher RA, Melnyk CW, Kelly KA, Dunn RM, Studholme DJ, et al. (2009) Uniparental expression of PolIV-dependent siRNAs in developing endosperm of *Arabidopsis*. Nature 460: 283–286.

73. Zhang X, Clarenz O, Cokus S, Bernatavichute YV, Pellegrini M, et al. (2007) Whole-genome analysis of histone H3 lysine 27 trimethylation in *Arabidopsis*. PLoS Biol 5: e129. doi:10.1371/journal.pbio.0050129.

74. Makarevich G, Villar C, Erilova A, Kohler C (2008) Mechanism of PHERES1 imprinting in *Arabidopsis*. Journal of Cell Science 121: 906–912.

75. Ngo QA, Moore JM, Baskar R, Grossniklaus U, Sundaresan V (2007) *Arabidopsis* GLAUCE promotes fertilization-independent endosperm development and expression of paternally inherited alleles. Development 134: 4107–4117.

76. Saze H, Mittelsten Scheid O, Paszkowski J (2003) Maintenance of CpG methylation is essential for epigenetic inheritance during plant gametogenesis. Nat Genet 34: 65–69.

77. Wang D, Tyson MD, Jackson SS, Yadegari R (2006) Partially redundant functions of two SET-domain polycomb-group proteins in controlling initiation of seed development in *Arabidopsis*. Proc Natl Acad Sci U S A 103: 13244–13249.

78. Zilberman D, Cao X, Jacobsen SE (2003) ARGONAUTE4 control of locus-specific siRNA accumulation and DNA and histone methylation. Science 299: 716–719.

79. Goodrich J, Puangsomlee P, Martin M, Long D, Meyerowitz EM, et al. (1997) A Polycomb-group gene regulates homeotic gene expression in *Arabidopsis*. Nature 386: 44–51.

80. Lindroth AM, Cao X, Jackson JP, Zilberman D, McCallum CM, et al. (2001) Requirement of CHROMOMETHYLASE3 for maintenance of CpXpG methylation. Science 292: 2077–2080.

81. Cao X, Jacobsen SE (2002) Role of the *Arabidopsis* DRM methyltransferases in de novo DNA methylation and gene silencing. Curr Biol 12: 1138–1144.

82. Murashige T, Skoog F (1962) A rewised medium for rapid growth and bioassays with tobacco tissue cultures. Physiologia Plantarum 15: 473–497.

83. Yang YH, Dudoit S, Luu P, Lin DM, Peng V, et al. (2002) Normalization for cDNA microarray data: a robust composite method addressing single and multiple slide systematic variation. Nucleic Acids Res 30: e15.

84. Smyth GK (2004) Linear models and empirical Bayes methods for assessing differential expression in microarray experiments. Stat Appl Genet Mol Biol 3: 1–25.

85. Storey JD (2002) A direct approach to false discovery rates. Journal of the Royal Statistical Society: Series B (Statistical Methodology) 64: 479–498.

86. Hulsen T, de Vlieg J, Alkema W (2008) BioVenn - a web application for the comparison and visualization of biological lists using area-proportional Venn diagrams. BMC Genomics 9: 488.

87. Curtis MD, Grossniklaus U (2003) A gateway cloning vector set for high-throughput functional analysis of genes in planta. Plant Physiol 133: 462–469.

88. Bent A (2006) *Arabidopsis thaliana* floral dip transformation method. Methods Mol Biol 343: 87–103.

89. Huang S, An YQ, McDowell JM, McKinney EC, Meagher RB (1997) The *Arabidopsis thaliana* ACT11 actin gene is strongly expressed in tissues of the emerging inflorescence, pollen, and developing ovules. Plant Mol Biol 33: 125–139.

90. Pfaffl MW (2001) A new mathematical model for relative quantification in real-time RT-PCR. Nucleic Acids Res 29: e45.